Fermi National Accelerator Laboratory

FERMILAB-Pub-91/101-A
May 1991

Investigating decoherence in a simple system

Andreas Albrecht
NASA/Fermilab Astrophysics Center
P.O.B. 500
Batavia, IL 60510

May 17, 1991

Abstract

I present the results of some simple calculations designed to study quantum decoherence. The physics of quantum decoherence is briefly reviewed, and then a very simple "toy" model is analyzed. Exact solutions are found using numerical techniques. The type of decoherence exhibited by the model can be changed by varying a coupling strength. I explain why the conventional approach to studying decoherence by checking the diagonality of the density matrix is not always adequate. Two other approaches, the decoherence functional and the Schmidt paths approach, are applied to the toy model and contrasted with each other. Possible problems with each are discussed.

1 Introduction

The physics of "quantum decoherence" plays an important role in our understanding of quantum mechanics. Quantum decoherence provides a mechanism whereby effects often attributed to "the collapse of the wave function" can arise in a system whose evolution is entirely unitary. This is accomplished by introducing a sufficiently complex "environment" into the calculation [1,2,3,4,5,6,7]. Such environments are present in most realistic

physical situations. Indeed, one finds that this mechanism is constantly in operation all around us, and decoherence is in large part responsible for the "state" in which we find many commonplace objects.

For example, one could never hope to observe a macroscopic pendulum in an energy eigenstate of its "harmonic oscillator" Hamiltonian, even if an initial state could be prepared that way [8]. Local interactions of the pendulum with its internal degrees of freedom, the gas in the room, or even just with the cosmic microwave background [9] would insure its rapid "collapse" into a much more localized state. This would be a consequence of correlations being set up with these other degrees of freedom which destroy the coherence of the initial state. At any given time the wavefunction of the world would then describe many localized copies of the pendulum, each at different positions, and each correlated with different environment states. The delocalized property of the initial state would just be reflected in these different positions being broadly distributed.

The physics of decoherence often points to the existence of preferred states, whose coherence is not destroyed by interactions with the environment. In the case of the pendulum these resemble the "coherent states", which are localized, and follow classical pendulum trajectories. Following the pioneering work of Zurek [2,3,4,6], the preferred states are often referred to as the "pointer basis". The word "pointer" is used because of the importance of the pointer basis in understanding measurement devices (many of which have pointers!). However (as Zurek and others have noted), the process of decoherence and the ability of special states to survive the decohering effects of the environment is a widespread phenomenon, and is not limited to man-made laboratory equipment. For many objects (such as the macroscopic pendulum) the pointer basis states are highly localized in both position and momentum. This fact can give rise to a classical treatment of these objects, in which both position and momentum are sharply defined.

The role of quantum decoherence in the early universe is of particular interest. It may provide valuable insights into questions relating to "initial conditions". One can ask which properties of the universe relate directly to the "initial state" and which are a consequence of dynamics forcing systems into the preferred pointer basis states. For example, in inflationary cosmology the state of the universe during inflation is a highly symmetric spatially homogeneous one. The fact that we observe an inhomogeneous

matter distribution today is attributable to local interactions destroying the coherence of this "initial" state [7] (see also [10,11,12,13,14]). The pointer basis states in this case are not homogeneous. Halliwell [15] has also emphasized the importance of quantum decoherence when studying emerging classical behavior in quantum cosmology.

There has recently been a lot of interest in the possible role that certain quantum gravity effects ("wormholes") could play as an environment responsible for decoherence [16,17,18,19,20,21,22,23]. In [24] Coleman argues that the decohering effects of the wormholes serve to define a particular pointer basis, (although he does not use that language). He shows that a state which is not of a particular type (not an "A-eigenstate") looses coherence, and may be thought of as separate A-eigenstates correlated with different "baby universe" states. The A-eigenstates, however, do not loose much coherence to wormhole interactions. This is analogous to the above discussion of the pendulum, and amounts to an argument that the A-eigenstates are the pointer basis induced by the wormhole interactions.

In familiar examples it is often easy to guess the nature of the pointer basis. For example, pointer basis states for the center of mass coordinates of macroscopic objects tend to be localized in space. This can be attributed to the locality of interactions with the environment. In addition, these localized states need to have fairly sharply defined momenta in order to remain localized in the course of time. Of course, there are notable exceptions to this rule. Superconducting Josephson junctions, for example, involves highly delocalized states which maintain their coherence [25,26,27].

In any case, when venturing into unfamiliar territory such as the early universe, one might want something more than heuristic arguments to work with. A common approach is to guess a pointer basis, and to check the diagonality of the reduced density matrix (in that basis) produced by tracing out over the environment. Care must be taken, however, for a number of reasons. For one, *any* density matrix can be diagonalized, but a pointer basis does not always exist. In many cases the decohering effects of the environment will rapidly destroy the coherence of any state. Secondly, I will show how non-zero off-diagonal elements can be tricky to interpret. They may correspond to small, stable fluctuations around a good pointer basis, or they may signal very noisy effects which prevent the emergence of a pointer basis.

There are two additional approaches which are discussed in the litera-

ture. The "decoherence functional" approach [28,29,30,31,32,33], and the "Schmidt Paths" approach [1,34,35]. The Schmidt paths approach is actually a straightforward extension of the diagonal density matrix idea. This paper is a study of these two points of view as applied to a simple system. The system has a parameter which can be adjusted to change the nature of the decoherence. Using the Schmidt point of view, I show that in some limits a static pointer basis emerges, while in other cases the pointer basis is dynamically evolving. In many cases the system is just noisy, and *no* state can survive the decohering effects of the environment. I note the possibility that in some of the noisy cases the Schmidt paths approach may loose some of its utility.

The decoherence functional is used to determine whether the wavefunction represents different histories for a given system which do not interfere with one another. When the answer is in the affirmative, the histories are said to be "decohering". Although closely related to the existence of a pointer basis, exhibiting decohering histories places more stringent demands on the physics. The calculations which I present illustrate how care must be taken in defining when these histories are "sufficiently decohering". Using one such criterion it appears that none of the examples studied here exhibit "decohering histories", due to the presence of fluctuations. None the less, some aspects of the history of the system may still be usefully discussed.

The next section is a review of the basic ideas of decoherence, and section 3 provides an introduction to the Schmidt paths point of view. In section 4 the toy model is introduced. In sections 5 and 6 the behavior of the toy model is analyzed from the Schmidt point of view. Section 7 starts with brief introduction to the decoherence functional, which is then used to analyse the toy model. Comparisons with previous work are made in section 8. Conclusions are presented in section 9. A number of technical issues are addressed in the appendices.

Throughout this paper I use units in which $\hbar = 1$.

2 Correlations and Decoherence

2.1 The exactly separable limit

Whenever one studies a system quantum mechanically, the wavefunction of the world, $|\psi\rangle_w$, is usually implicitly assumed to have the following direct product form:

$$|\psi\rangle_w = |\psi\rangle_s \otimes |\psi\rangle_r . \tag{1}$$

Here $|\psi\rangle_s$ is the wave function of the *system* under study, and $|\psi\rangle_r$ is a state for the *rest* of the degrees of freedom of the world, which do not concern the particular calculation at hand. In fact, one usually further assumes that $|\psi\rangle_s$ itself can be written as a direct product:

$$|\psi\rangle_s = |\psi\rangle_1 \otimes |\psi\rangle_2 \otimes |\psi\rangle_3 \otimes ... |\psi\rangle_n \otimes ... \tag{2}$$

The subscripts indicate the numerous subsystems into which one divides the "system under consideration". These subsystems may be an incoming particle, a target, a clock, etc..

The product form for a wavefunction is far from general, and one might wonder why, instead of Eq (1), one is not forced to consider the more general case:

$$|\psi\rangle_w = \sum_{i,j} \alpha_{i,j} |i\rangle_s \otimes |j\rangle_r \tag{3}$$

where $\{|i\rangle_s\}$ and $\{|j\rangle_r\}$ are bases which span the Hilbert spaces of the "system" and the "rest of the world" respectively. One could just embrace the product form as one of the initial assumptions, but there is another point of view which is much more physically motivated. This second point of view is closely tied with the notion of "quantum decoherence" and is the subject of this paper. I will start the discussion with some formal remarks, and then bring in the additional complications which make the picture more interesting and physical.

In order to exactly preserve the product form of Eq (1) the total Hamiltonian must generally be of the form:

$$H_w = H_s \otimes I_r + I_s \otimes H_r \tag{4}$$

where I represents the identity operator in the labeled subspace [1].

[1] Another possibility is that $|\psi\rangle_s \otimes |\psi\rangle_r$ is an eigenstate of the total Hamiltonian. This possibility will be relevant to later discussion.

However, given a separable Hamiltonian, one could go beyond the simple product form of Eq (1), and instead have:

$$|\psi\rangle_w = \sum_i \alpha_i |\psi_i\rangle_s \otimes |\psi_i\rangle_r \tag{5}$$

Then, as long as

$${}_r\langle\psi_i|\psi_j\rangle_r = \delta_{i,j} \tag{6}$$

each $|\psi_i\rangle_s$ will evolve independently according to H_s, and there will be no interference among them. Note that there is only one summation in Eq (5), so each state $|\psi_i\rangle_s$ is uniquely correlated with its own member of the orthonormal set $|\psi_i\rangle_r$. The lack of interference between the different $|\psi_i\rangle_s$ states can be seen by considering any operator with non-zero matrix elements between the different $|\psi_i\rangle_s$'s, and which operates entirely in the "*system*" subspace. One can write such an operator as $\hat{O}_s \otimes I_r$. The operator $\hat{O}_s$ could represent a third system measuring the system in question. The ability of $\hat{O}$ to mix different $|\psi_i\rangle_s$'s would suggest the interference could be observed among the different terms in $|\psi\rangle_w$. However, when one looks at the situation in the full Hilbert space one finds that

$$\begin{aligned} {}_w\langle\psi|\,\hat{O}_s \otimes I_r\,|\psi\rangle_w &= \sum_{i,j} \alpha_i^* \alpha_j \; {}_r\langle\psi_i \mid \psi_j\rangle_r \, {}_s\langle\psi_i|\,\hat{O}_s\,|\psi_j\rangle_s & (7) \\ &= \sum_i \alpha_i^* \alpha_i {}_s\langle\psi_i|\,\hat{O}_s\,|\psi_i\rangle_s \,. & (8) \end{aligned}$$

Here we see that the othogonality of the states in the r subspace prevents $\hat{O}_s$ from mixing different $|\psi_i\rangle_s$'s.

What I have just described is an idealized example of the important role correlations can play in quantum physics. I have shown how the presence of correlations with an "environment" can allow a wavefunction to describe a multitude of different non-interfering histories for a system. (In this case the histories are given by the time evolution of the $|\psi_i\rangle_s$'s). This basic mechanism allows one to reproduce effects often attributed to the "collapse of the wavefunction", where no interference is observed between different "outcomes" of a quantum measurement. To properly illustrate this point one needs to expand the picture, so that each non-interfering history includes many subsystems which can interact with one another (see for example [3,35]).

An additional point I should make here is that one normally assigns probabilities to the different independent terms, corresponding to the probabilities of the different "outcomes". For sensible probabilities to be assigned, one needs the states of the system in Eq 5 to also obey (at least to a very good approximation) an orthonormality relation:

$$ {}_s\langle\psi_i|\psi_j\rangle_s = \delta_{i,j}, \tag{9} $$

just as the $|\psi_j\rangle_r$ do. This is needed because, to the extent that the different $|\psi_i\rangle_s$'s do overlap, they do not represent distinct physical situations, and the probabilities ones assigns to each will necessarily not add to unity. [2]

2.2 Interactions and the origin of the correlations

This discussion has been focused on correlations between the system and the "*rest*" subspaces. So far, I have had nothing to say about the origin of these correlations. Because of the exact separability assumed for the Hamiltonian, the correlations are not a result of dynamics, but are just a property of the initial state which is preserved by the dynamics.

The reason these considerations are interesting, however, is that in the physical world one never has *exact* separability. While there are cases which are separable enough from a practical point of view, there are often ways we can manipulate the situation to expose the additional degrees of freedom (or subspaces), and to exhibit interactions among different $|\psi_i\rangle$'s in a wavefunction of the form Eq 5. (In some interesting cases, including in an example I will present in this paper, the interaction between system and environment will actually dominate over the respective self Hamiltonians.)

An important example is that of the "quantum measurement". A decaying nucleus can interact with a Geiger counter, setting up correlations with its internal degrees of freedom. Afterwards, the total wavefunction can be thought of as having two essentially independent terms, one describing the case where the Geiger counter has clicked, and the other where it has not clicked. In this case, the lack of exact separability allows one to associate the creation of the relevant correlations with the interactions between the decay products and the Geiger counter.

[2] This constraint also removes some ambiguities that were present in the rather formal discussion so far (there are *many* different expansions of a given wavefunction which conform with just Eqs 5 and 6).

There has been a lot of theoretical work linking quantum measurement with the setting up of correlations such as those discussed above. I refer the reader to [1,3,9] for further discussion.

With the abandonment of exact separability, one is able to point to a physical origin for correlations under discussion. However, confusion sometimes arises as to how the correlations are to be discussed. For example, the specially correlated form for the wavefunction (Eq 5) is not generally preserved under time evolution unless the Hamiltonian is exactly separable. In a typical discussion one often sees

$$|\psi\rangle_w \approx \sum_i \alpha_i |\psi_i\rangle_s \otimes |\psi_i\rangle_r \tag{10}$$

and

$${}_r\langle\psi_i|\psi_j\rangle_r \approx {}_s\langle\psi_i|\psi_j\rangle_s \approx \delta_{i,j} \tag{11}$$

which are just Eqs (5), (6), and (9) with $\approx$ replacing $=$. These equations are ambiguous and one is then left with a number of questions. For example: How close to equality is "good enough" in each of these expressions.

3 The Schmidt Paths

In the standard approach, one studies

$$\rho_s \equiv \mathbf{tr}_r \rho_w, \tag{12}$$

where one has traced out the *rest* space in ρ_w ($\equiv |\psi\rangle\langle\psi|$) to produce the reduced density matrix for the *system*. One notes that if $|\psi\rangle_w$ takes on the specially correlated form (Eq (5)) then:

$$\rho_s = \sum_{ij} |\psi_i\rangle_s \alpha_i^* \alpha_j {}_s\langle\psi_j| \times {}_r\langle\psi_i \,|\, \psi_j\rangle_r \tag{13}$$

$$= \sum_i |\psi_i\rangle_s \alpha_i^* \alpha_i {}_s\langle\psi_i|\,, \tag{14}$$

and the density matrix for the system is diagonal.

It is quite common to then reverse the argument, and say that if the density matrix is found to be diagonal in a particular basis, then it is these basis states which are specially correlated with the environment. However,

any density matrix can be diagonalized, so a diagonal density matrix alone does not tell you very much.

In fact, it turns out that the "specially correlated" form of the wavefunction (Eq (5)) is actually completely general, even when the orthogonality relations (Eqs (6) and (9)) are satisfied for both subsystems. This is an old result due to Schmidt [36], and is related to the fact that in addition to ρ_s one can construct

$$\rho_r \equiv \mathbf{tr}_s \rho_w. \tag{15}$$

Both ρ_s and ρ_r can be diagonalized. As long as the world is in a pure state, i.e.

$$\rho_w = |\psi\rangle \langle\psi| , \tag{16}$$

both density matrices will have *identical* eigenvalues. The one corresponding to the larger Hilbert space will have additional zero eigenvalues. (The case where ρ_w is not pure can be treated in a similar way, as discussed in [35].)

A basis for the whole Hilbert space can be formed as the direct product space of the eigenstates of the two density matrices. When the state of the world is expanded in this direct product basis one finds

$$|\psi\rangle_w = \sum_i \sqrt{p_i}\, |i\rangle_s^S\, |i\rangle_r^S , \tag{17}$$

where the $|i\rangle_s^S$ and $|i\rangle_r^S$ denote the eigenstates (or "Schmidt states") corresponding to the non-zero eigenvalues, p_i of each density matrix. Phase information can be incorporated into the the eigenstates to allow positive real values for the expansion coefficients $\sqrt{p_i}$.

Equation (17) shows that given a $|\psi\rangle_w$, and a particular direct product form for the Hilbert space, the "specially correlated" form of Eq (5) may always be exactly obtained using the Schmidt procedure. In general, however, time evolution will not preserve this form, and the Schmidt decomposition must be re-calculated at each moment of time. People are often surprised by the Schmidt result. Appendix A gives a brief proof, and further discussion designed to give the result more intuitive appeal.

By nature, the Schmidt form of a state gives an exact account of the correlations present between any two subsystems. (Each $|i\rangle_s^S$ is uniquely correlated with its own $|i\rangle_r^S$.) That makes it a natural starting point for a discussion of decoherence. A particular application of interest here is

the search for a pointer basis. That means determining if there are any states for the systems whose coherence is not continually destroyed by the setting up of correlations with the environment. The Schmidt states will in general vary in some crazy way with time, as $|\psi\rangle_w$ evolves, indicating ever-changing correlations between the system and the environment. My favorite approach to the search for a pointer basis is to follow the evolution of the Schmidt states (which trace out "Schmidt paths"). When their evolution becomes sufficiently regular, on can say that they represent a pointer basis. A version of this point of view was first proposed by Zeh [1], and has been further discussed in [34,37,35,38,39]. (I disagree with some of the statements made in [38], see [39]) If one wishes to see the Schmidt paths point of view carefully spelled out, I direct you to Refs [1,35].

For this article, I move right along to some simple examples, which might be the best way to be introduced to these ideas. I turn now to the description of a simple "toy system", with which calculation are easy, yet for which the decohering behavior can be adjusted by varying a parameter. The Schmidt paths point of view will be used to analyse the system. Then another perspective on decoherence, the "decoherence functional" will be reviewed and applied to the same system.

4 The toy system

The system which I study is designed to exhibit decoherence in a primitive form, with as little extra baggage as possible. The world is divided into a two state subsystem (subsystem number 2) coupled to an "environment" of variable size, n_1 (subsystem number 1). Thus, the Hilbert space of the "world" is $2n_1$ dimensional. The Hamiltonian can be written

$$H = H_1 \otimes I_2 + I_1 \otimes H_2 + H_I \tag{18}$$

Where I_k represent the unit operator in the space of subsystem k. the first two terms represent the self Hamiltonians of the environment and system respectively, and the last term gives the interactions between system and environment. I choose the self Hamiltonian of the two state system to be

$$H_2 = E_2 \cdot (\, |\uparrow\rangle\langle\downarrow| \; + \; |\downarrow\rangle\langle\uparrow| \,) \, . \tag{19}$$

This causes the spin to rotate, from the point of view of the $\{|\uparrow\rangle, |\downarrow\rangle\}$ basis, with a frequency proportional to E_2. The self Hamiltonian of system 1 (the "environment") is

$$H_1 = E_1 \times \hat{R} \tag{20}$$

where $\hat{R}$ is an Hermitian matrix with the real and imaginary parts of each independent matrix element chosen randomly in the interval $[-0.5, 0.5)$ (by the computer's random number generator).

It is important for the physics which I want to study that the environment (subsystem 1) evolve in a way which exhibits no special relationship with the "system" (subsystem 2). The random form of H_1 insures this, without trying to mimic any particular physical environment.

In a similar spirit, the interaction Hamiltonian is:

$$H_I = E_I \times \left(|\uparrow\rangle \langle\uparrow| \otimes H_1^{\uparrow} \;\; + \;\; |\downarrow\rangle \langle\downarrow| \otimes H_1^{\downarrow} \right). \tag{21}$$

The matrices $H_1^{\uparrow}$ and $H_1^{\downarrow}$ are each different random matrices constructed in the same fashion as $\hat{R}$. The idea of this interaction is to set up different correlations between the system and the environment depending on whether the spin is up or down. If the spin is up, the first term in H_I causes the environment state to be pushed in one direction (in its Hilbert space), while if the spin is down, the second term pushes the environment in another direction. In this sense the interaction can be thought of as providing for a primitive "measurement", with the $\{|\uparrow\rangle, |\downarrow\rangle\}$ basis being the "pointer basis" in which the measurement occurs. However, although the two different random H_1's insure that the environment is pushed in the two different directions in each of the $|\uparrow\rangle$ versus $|\downarrow\rangle$ cases, there is purposely no attempt to attach any additional interpretation to $H_1^{\uparrow}$ and $H_1^{\downarrow}$. I have made this choice in order to keep the discussion focused on the simplest possible example.

In real physical examples of decoherence the environment may or may not be as "anonymous" as I have depicted it here. In some cases a real laboratory measurement is being performed, and we would easily identify some subsystem of the environment as a "pointer" or a mark in a lab notebook, which has become correlated with the state of the system under examination. In other cases the role of the environment may be played by a photon scattering off the object in question, and propagating off into "empty" space. In this second situation one would have a fairly clear idea of the state of the photon (at least until it interacted with a dust particle

or star!). In yet other cases decoherence can be caused by interactions with some sort of thermal bath (such as the earth's atmosphere). In such a case one only has a very rough idea of the specific states of the environment that become correlated with the system, and the situation begins to resemble the one I have set up here. In each of these cases, an essential ingredient is that the interactions serve to set up correlations between the system and environment in a particular way. It is this feature which I have sought to incorporate here, while keeping specific details to a minimum.

The reader may notice a similarity between this system and others that have appeared in the literature on quantum decoherence. I will save until section 8 a discussion of the relationship between this and other work.

5 Calculating Schmidt paths

The calculations I undertake are quite simple. I use a computer program (described in appendix B) to evolve an initial state unitarily under the action of the Hamiltonian presented in the previous section. The density matrix for system 2 (ρ_2) is easily constructed at any time by tracing over the system 1 subspace (the "environment"). The density matrix is diagonalized, and the Schmidt paths, described by the time history of the eigenvectors, can be followed. This process has been repeated for a variety of initial states, and for different relative strengths of the couplings E_1, E_2, and E_I in the Hamiltonian.

5.1 Weak coupling

I start the discussion with the following case: The parameters of the Hamiltonian are

$$E_1 = 1, \quad E_2 = 1, \quad E_I = .3\,. \tag{22}$$

This represents weak coupling, since the self-energies of systems 1 and 2, (E_1, and E_2) are higher than the interaction energy (E_I). The initial state is

$$|\psi(\text{intial})\rangle = |\uparrow\rangle \otimes |\text{random}\rangle_1\,, \tag{23}$$

where $|\text{random}\rangle_1$ is a state chosen randomly in the environment subspace. The random state is generated by choosing both the real and imaginary

parts of its expansion coefficients in the working basis randomly on the interval $[-0.5, 0.5)$ and then normalizing (See Appendix B for further details). Figure 1 displays a variety of information about this example. The dotted curve on the lower plot represents the entropy of the system, in units where the maximum entropy is unity:

$$S \equiv -\mathbf{tr}\left(\rho\left(log_2\rho\right)\right). \tag{24}$$

Note how the initial entropy is zero. Because the initial state (Eq 23) has a simple direct product form, the individual subsystems are in "pure" states, the density matrix has only one non-zero eigenvalue, and the entropy is zero. Naturally enough, the entropy increases with time. The solid line on the lower plot shows the value of the larger eigenvalue of ρ_2. Since there are only two eigenvalues, this curve contains no more information than the entropy (one can be calculated form the other), but it is handy to have both forms of the information available.

It is important to remember that the whole "world" remains in a pure state throughout the evolution. It is just relative to the subdivision into spin system and environment that the density matrix becomes "mixed", and the entropy becomes non-zero.

The dotted line on the top plot in Fig (1) gives the expectation value of the spin operator $I_1 \otimes \hat{J}$ where

$$\hat{J} \equiv |\uparrow\rangle \left(+\frac{1}{2}\right) \langle\uparrow| \;+\; |\downarrow\rangle \left(-\frac{1}{2}\right) \langle\downarrow|. \tag{25}$$

This curve starts at $1/2$, as it should given that the initial state is pure "$|\uparrow\rangle$", and oscillates with the period π, corresponding to the self-Hamiltonian of system 2. However, the amplitude of the oscillation declines with time. This coincides with the increasing entropy, and is indicative of the fact that the spin system is no longer in a pure state. To the extent that the spin is not definitely in a particular state, the quantity

$$_w\langle\psi|\, I_1 \otimes \hat{J}\, |\psi\rangle_w \tag{26}$$

will not clearly exhibit the evolution of a pure spin state.

The solid curve in the top box of Fig (1) represents the expectation value of the spin in one of the eigenstates of ρ_2 (the one corresponding to the larger of the two eigenvalues). This quantity allows one to follow one of

the two "Schmidt paths" associated with the two state system. This curve also exhibits the oscillatory behavior induced by the self-Hamiltonian. An important feature of the solid curve is that the amplitude remains steady. There is no sign that the clean oscillatory behavior is degrading with time, as it is with the dotted curve. This fact allows one to regard the oscillating states as a pointer basis. The wavefunction describes two possible paths for the spin, each oscillating, but with different phases. The decohering effect of the environment does not dramatically effect the evolution of the oscillating states.

5.2 What does it mean?

In order to ascribe physical meaning to these results on must speak about how other systems interact with the spin system. If one were to adhere strictly to the spirit of this work, one would need to enlarge the Hilbert space so as to include the additional systems. I will not do that here, but instead describe in words what might be expected. (Reference [35] discusses how to extend the Schmidt approach to multiple subsystems.)

The results in Fig 1 can be taken to mean the following: If one were to interact with the spin system with an apparatus which couples only to the spin, and not to the environment, then one may treat the spin as being on two different paths. On each path the spin is oscillating, but the paths are 180 degrees out of phase. At any given time, interference between the two paths could never be detected, due to the correlations with the environment. Any interaction just with the spin can be represent by an operator of the form $\hat{O}_s \otimes I_r$. The absence of interference is evident by the inability for such an operator to mix the spin states on the different paths, as illustrated in Eq 8.

There is a sense in which one would want to have the probability for each path be constant, in order to think of the paths as not interfering with one another in the course of time. The probability shown in Fig 1 (solid curve, bottom plot) is never exactly constant, and in the first half of the time period, shows a trend downward. I discuss this issue further in Section 7 and in [39]. For now, I just remark that in realistic situations the probability can never be expected to be exactly constant. In cases where the probability is changing sufficiently slowly, one can think of reasonably separate paths which are slowly branching into one another due to fluctuations.

The (oscillating) "state" of the spin is determined by the dynamics. The only property which is determined by the state of the "world" is the relative probability of finding the spin with one phase or another. This way in which correlations, rather than just the intial conditions, determine the "state" in which we find a system is of particular interest in the field of cosmology. In cosmology one is driven to contemplate the "initial conditions of the universe". It is very important however, that we clarify what properties of our universe are a reflection of the initial conditions, and which properties are the result of correlations set up by the dynamics, and the nature of the particular measurements we are able to make. (Of course such effects may also be related in some less direct way to the initial conditions.)

5.3 Strong coupling

I now vary the problem by increasing the strength of the interaction, relative to the self-Hamiltonians. Figure 2 describes a situation identical to that in Fig 1, except that now

$$E_1 = 1, \quad E_2 = 1, \quad E_I = 1 \, . \tag{27}$$

Although there are some traces of the periodicity present in the previous case, the clean effect is completely gone. The is no clear pointer basis in this case. One could say that whatever states are specially correlated with the environment at one time, the interactions always decohere them. One is left no chance to view the evolution of the spin system in a simple way. Note that the entropy increases much more rapidly than in Fig 1, in keeping with the disordered nature of the more strongly coupled case.

For Fig 3, the interaction strength has been increased to $E_I = 3$. Again, there is no simple behavior on the part of the Schmidt paths, but there is a new feature: The plotted Schmidt path is now more likely to be spin up, than spin down.

This feature becomes more pronounced as the interaction strength is increased further. Figure 4 shows the case where $E_I = 10$. In this case the two Schmidt paths are very closely pinned to spin up (shown) and spin down (orthogonal to the one shown). The paths are now constant in time, except for small fluctuations. One can again say that there is a pointer basis, but it is a different one, as compared with the weakly coupled, oscillating case.

Now one can say that the wave function of the world exhibits two paths, or histories, for the spin. One is constant spin up. The other is constant spin down.

One might wonder how the Schmidt analysis compares with the standard approach of just looking at the diagonality of the the density matrix. Fig 5 shows the magnitude of the off-diagonal element, $\langle\uparrow|\,\rho_2\,|\downarrow\rangle$ in the strongly coupled (dashed curve) and medium coupled (solid curve) cases. The size of this quantity is indeed smaller in the strongly coupled case, corresponding to the fact that $\{|\uparrow\rangle, |\downarrow\rangle\}$ is a good pointer basis in that case. However, the difference is not striking, and one may not have even noticed the dramatic differences between the two cases if $\langle\uparrow|\,\rho_2\,|\downarrow\rangle$ was all that was studied.

5.4 The Watchdog effect

The strongly coupled case gives a nice illustration of the "watchdog effect" whereby frequent measurement of a system in a particular state can prevent it from evolving [40,41,42,43]. I argued in section 4 that the environment (system 1) plays the role of a primitive measurement apparatus. Increasing the interaction strength decreases the time it takes for correlations to be set up with the environment, and thus increases the frequency with which the "measurements" take place. The spin is measured in the $\{|\uparrow\rangle, |\downarrow\rangle\}$ basis. When the frequency of measurement is increased (by increasing E_I) the spin is prevented from evolving out of these states, as exhibited by the constant Schmidt paths.[3]

I find this illustration of the watchdog effect appealing, since (as in [43]) the measurements are not represented by projection operators. Projection operators are often a perfectly adequate way of representing a measurement, when one wants to simplify the problem by not including the measurement apparatus in the total wavefunction. However, in a presentation of the watchdog effect the measurement is the focus of the discussion. It can be misleading when something as mathematical and remote as a projection operator plays such central role. When representing measurements with projection operators, it might appear that an increased frequency of

[3]The idea that the environment can often provide the "measurements" necessary for the watchdog effect has been discussed in the literature [4,9]

measurement can be had "for free", and the corresponding change in the dynamics can appear mysterious. In the above discussion, one can identify the increased frequency of measurement with an interaction becoming stronger. It is not surprising that in the presence of a very strong interaction the system behaves differently.

6 The high entropy case

So far I have discussed only direct product initial states, which have zero entropy. In the situations where a nice pointer basis appeared the entropy never really got very large and, correspondingly, there was always one eigenvalue of the density matrix which was clearly the largest. I now shift the discussion to higher entropy states

6.1 Strong coupling

In the strongly coupled case (Fig 4), the initial state was pure spin up, and the evolution was one in which $|\uparrow\rangle$ states remained stable. It is not surprising that the world does not deviated too far from its low entropy initial state. Figure 6 shows the same system as Fig 4, but viewed much later in its evolution. One can see that the entropy has increased somewhat, but it still is far from maximal. The Schmidt path evolution has not changed much, although the fluctuations look a bit larger. I have found that the picture looks similar to Fig 6 even at times a factor of ten larger.

However, one can just start with a higher entropy initial state, and see how the Schmidt paths behave. One might expect that if the coupling were strong, the same simple evolution would be obtained. Figure 7 shows the results from a calculation that started with "random initial conditions". Specifically, I consider the expansion of the initial wavefunction in the energy eigenstate basis (eigenstates of the total Hamiltonian) and choose the real and imaginary parts of each coefficient randomly on the interval $[-0.5, 0.5)$, and then normalize. Note how the entropy is initially close to maximal, as would be expected. The Schmidt paths clearly do not reproduce the simple constant spin (up or down) evolution of the low entropy case. One does see some long time features (on time scales $O(10)$) which might suggest a tendency toward constant behavior, but that is far

from clear.

Perhaps the high entropy case needs a larger coupling to achieve the simple constant spin pointer basis evolution. Figure 8 shows the results of increasing the relative strength of the interaction even more ($E_I/E_2 = E_I/E_1 = 10^7$), and starting with the same initial state. The behavior of the Schmidt paths in this case is even more remote from the low entropy paths.

What we are seeing here might be related to the definition of the Schmidt paths. Schmidt paths are based on the eigenvectors of the density matrix ρ_2. The high entropy case corresponds to the eigenvalues of ρ_2 being nearly degenerate (note how the larger of the two eigenvalues, given by the solid line in the lower plot, is close to 1/2). When the eigenvalues of a matrix are exactly degenerate, the eigenvectors are not uniquely specified. It seems reasonable that when the eigenvalues are close to degenerate, the eigenvectors depend in a delicate way on small fluctuations in the elements of ρ_2. This dependence on small fluctuations appears to be washing out the nice pointer basis behavior exhibited by the low entropy case.

While this explanation seems reasonable, it raises troubling questions about the ability of the Schmidt paths to identify a pointer basis in realistic physical situations. For example, one should be able to construct an experiment where the probability that a Geiger counter has ticked is as close to 1/2 as one might want. There should be no confusion about the existence of two non-interfering paths in that situation. Certainly there has been no observed degradation of Geiger counter performance in that limit.

6.2 Weak coupling

I now turn to the case of high entropy, weakly coupled systems. Figure 9 shows the results of using the same high entropy initial state as above but now with

$$E_1 = 1, \quad E_2 = 1, \quad E_I = .3\,. \tag{28}$$

The story appears to be similar to the strongly coupled case. Although there are vestiges of the oscillating behavior observed in the low entropy states (compare with Fig 1), the evolution is not as clean, and it is clear that the same type of pointer basis behavior is not present.

Figure 10 shows the same arrangement as in Fig 1 (weak coupling, with

low initial entropy), viewed much later in its evolution. As with the strongly coupled case, the early behavior of the Schmidt paths persists at later times. (Actually there does appear to be some modulation of the amplitude here, but the effect is limited, and it may be attributable to the small size of the environment.) What is interesting is that in this case the entropy is very high, at least as high as the entropy in the case of random initial conditions (Fig 9). I take this as something of an "existence proof" that the Schmidt paths can identify a pointer basis in a situation where density matrix eigenvalues are nearly degenerate. The evolution of the Schmidt paths need not be dominated by the fluctuations in this limit.

The analogy here with the Geiger counter is interesting. There are physical situations where the fact that the entropy is high prevents a pointer basis from emerging. For example, if a Geiger counter is placed in a furnace, it is no longer a useful measurement device. It is interesting that in the Geiger counter case, the situation where simple pointer basis behavior is destroyed (in the furnace) is where the interaction with the environment is strong, just as in my calculations. In situations where a Geiger counter is expected to handle degenerate probabilities without a problem, its evolution is dominated by its self interactions. This is just the situation where I was able to observe coherent pointer basis behavior under high entropy in my simple system. This is encouraging, but more work needs to be done. The question of whether the Schmidt paths are a good way of looking at the physics in situations with nearly degenerate probabilities has yet to be clearly resolved.

It is intriguing that Figures 9 and 10 both show (pure) states with have high entropy from the point of view of the spin-environment subdivision. Although the entropy is similar, the states have very different behavior. One was chosen randomly, and the other was reached by evolving a particular low entropy initial state for a long time. A more thorough investigation of the differences between these two states is currently underway.

6.3 Quantum measurement

It would be nice to use these calculations to illustrate the "collapse" of the wave function associated with a quantum measurement. In principle one

would do this buy setting up an intial state of the form:

$$|\psi(\text{initial})\rangle_w = \left(\frac{|\uparrow\rangle + |\downarrow\rangle}{\sqrt{2}}\right) \otimes |\text{something}\rangle_1 \tag{29}$$

and tracing the evolution of the Schmidt paths. Initially one Schmidt state would be $(|\uparrow\rangle + |\downarrow\rangle)/\sqrt{2}$. In the strongly coupled case, as time progressed, one could simply watch the evolution of this schmidt path and watch the state "collapse" into a $|\uparrow\rangle$ or $|\downarrow\rangle$ state. At the same time of course, the other Schmidt path would have its probability increasing from zero, and would become peaked around the other alternative.

The catch is, at least when the initial states of the environment are the random ones I choose here, that the final state is identical to the state of the high entropy, strong coupling case already discussed. (One can see this because the two paths should end up with roughly equal probabilities, and that means high entropy.) Thus the outcome is not two nice $|\uparrow\rangle$ and $|\downarrow\rangle$ Schmidt paths. This might not be too surprising since a random initial state for the environment makes it a very noisy measurement apparatus. I am presently investigating the possibility of properly "preparing" the environment in a suitable initial state so as to make it work like a good measurement apparatus in this example. It is possible however, that my toy system is too simplistic to play that role.

7 The decoherence functional

7.1 Review of the decoherence functional

The Schmidt paths can be thought of as a set of different paths or histories followed by the spin. There is another approach to identifying histories, called the decoherence functional approach [28,29,30,31,32,33]. The basic idea is that if the wave function contains a number of different terms, each describing an independently evolving path, then it can not hurt to project out all but one term. If the evolution is truly independent, the remaining term should evolve the same way, regardless of whether the projection is made. If a path survives this test, it is said to be "decohering", and a probability can be assigned to that particular path.

As an example, I will consider the constant spin up path, and investigate whether it "decoheres" according to the decoherence functional. The first step in using the decoherence functional is to construct what I call the "path projected states". That is, one evolves the initial state in time, while periodically projecting onto the path. The path projected state of the spin-up path, written $|[\uparrow\uparrow \ldots \uparrow]\rangle$, is

$$|[\uparrow\uparrow \ldots \uparrow]\rangle \equiv \hat{P}_{\uparrow} e^{-iH_w(t_n - t_{n-1})} \ldots \hat{P}_{\uparrow} e^{-iH_w(t_2 - t_1)} \hat{P}_{\uparrow} e^{-iH_w(t_1 - t_0)} |\psi\rangle \qquad (30)$$

where

$$\hat{P}_{\uparrow} \equiv |\uparrow\rangle \langle\uparrow| \otimes I_1. \qquad (31)$$

The times $\{t_i\}$, when the projections are performed, are an important part of the definition of the path and represent a "coarse graining in time". Changing the $\{t_i\}$ results in a "different" path.

One then constructs different path projected states corresponding to deviations from the constant spin up path. For example,

$$|[\uparrow \ldots \uparrow\downarrow\uparrow]\rangle \equiv \hat{P}_{\uparrow} e^{-iH_w(t_n - t_{n-1})} \ldots \hat{P}_{\uparrow} e^{-iH_w(t_3 - t_2)} \hat{P}_{\downarrow} e^{-iH_w(t_2 - t_1)} \hat{P}_{\uparrow} e^{-iH_w(t_1 - t_0)} |\psi\rangle \qquad (32)$$

corresponds to a path where the spin just flips to down at one time, and otherwise remains up.

In order to determine if a given path decoheres, one considers the path projected states corresponding to all possible deviations from the given path. One checks their overlap with the original path projected state, and to the extent that the overlap is small, the path is said to decohere. The direct products of two different path projected states are called the off-diagonal elements of the decoherence functional. The magnitude squared of the path projected state corresponding to the given path (or the "on-diagonal element of the decoherence functional") gives the probability for that path, if that path decoheres.

The set of "all possible paths" is constructed by making all possible choices for the projection operator at each time from a "complete" set of projection operators which includes the projection used in the initial path. Complete means that the projections in the set sum to the identity. The paths are also taken to be exclusive, so that no two projections overlap.

7.2 Calculating with the toy system

In the simple example considered here, the only way to make a path alternate to "constant $\uparrow$" is to project onto $|\downarrow\rangle$ at some times instead. Table 1 shows selected elements of the decoherence functional calculated for the toy model under study. The left column gives results for the strongly coupled case, where $E_1 = E_2 = 1$ and $E_I = 10$. The time between projections, Δt, is 0.2 in this case. The initial conditions were $|\uparrow\rangle \otimes |\text{random}\rangle$, and the situation is identical to the case described in Fig 4 from the Schmidt point of view. The Schmidt analysis suggested that the spin follows constant spin paths, aside from small fluctuations. This seems to be born out nicely by the decoherence functional. The off-diagonal elements are small, and the on-diagonal elements are large, giving a substantial probability to the constant spin up path. Here I provide the magnitude of the real part of the off-diagonal elements. In some discussions of the decoherence functional it is the real part which is given importance [28]. I have found both the real and imaginary parts to be close in size, as suggested in [32].

The right hand column of Table 1 corresponds to the medium coupling case pictured in Fig 2 from the Schmidt point of view. Everything is the same as the strongly coupled example except in this case I take $E_I = 1$. Neither the plots in Fig 2, nor an inspection of the the Hamiltonian lead one to expect the spin can have any clear history assigned to it. Certainly there is no clear indication that a pointer basis should emerge. However, the qualitative feature of the two columns in Table 1 are much the same. It is true that the off-diagonal elements are larger in the medium coupled case, as compared with strong coupling, but in all cases they are small compared with unity.

Tables 2 and 3 give the same quantities as Table 1, but for different values of Δt, the time between projections. In these examples the off-diagonal elements show even less of a clean distinction been the strong and medium coupled cases. The origin of the uniformly small off-diagonal elements is this: Each path projected state is a vector in a large space. It is a very special case for two vectors in a large space to have significant overlap. It is easy for even the "random" dynamics of the medium coupled case to result in path projected states which have little overlap.

The off-diagonal elements of the decoherence functional showed very little difference, when comparing the strong versus medium coupled cases.

Elements of the Decoherence Functional
$\Delta t = 0.2$

$E_I = 10$			$E_I = 1$		
$\langle[\uparrow\uparrow]\|[\uparrow\uparrow]\rangle$	=	0.96	$\langle[\uparrow\uparrow]\|[\uparrow\uparrow]\rangle$	=	0.92
$\|\Re\langle[\uparrow\uparrow]\|[\downarrow\uparrow]\rangle\|$	=	0.0016	$\|\Re\langle[\uparrow\uparrow]\|[\downarrow\uparrow]\rangle\|$	=	0.034
$\langle[\uparrow\uparrow\uparrow\uparrow\uparrow\uparrow]\|[\uparrow\uparrow\uparrow\uparrow\uparrow\uparrow]\rangle$	=	0.88	$\langle[\uparrow\uparrow\uparrow\uparrow\uparrow\uparrow]\|[\uparrow\uparrow\uparrow\uparrow\uparrow\uparrow]\rangle$	=	0.79
$\|\Re\langle[\uparrow\uparrow\uparrow\uparrow\uparrow\uparrow]\|[\uparrow\uparrow\downarrow\uparrow\uparrow\uparrow]\rangle\|$	=	0.0043	$\|\Re\langle[\uparrow\uparrow\uparrow\uparrow\uparrow\uparrow]\|[\uparrow\uparrow\downarrow\uparrow\uparrow\uparrow]\rangle\|$	=	0.029
$\|\Re\langle[\uparrow\uparrow\uparrow\uparrow\uparrow\uparrow]\|[\downarrow\uparrow\downarrow\uparrow\downarrow\uparrow]\rangle\|$	=	1.7×10^{-7}	$\|\Re\langle[\uparrow\uparrow\uparrow\uparrow\uparrow\uparrow]\|[\downarrow\uparrow\downarrow\uparrow\downarrow\uparrow]\rangle\|$	=	2.9×10^{-5}

Table 1: Some elements of the decoherence functional. The quantity $\Delta t = 0.2$ refers to the time between projections. Entries in the $E_I = 10$ column come from the same initial conditions and coupling strengths as the case presented in Fig 4 from the Schmidt point of view. The $E_I = 1$ column corresponds to Fig 2.

Elements of the Decoherence Functional

$\Delta t = 1$

$E_I = 10$		$E_I = 1$	
$\langle[\uparrow\uparrow]\|[\uparrow\uparrow]\rangle$	$= 0.75$	$\langle[\uparrow\uparrow]\|[\uparrow\uparrow]\rangle$	$= 0.22$
$\|\Re\langle[\uparrow\uparrow]\|[\downarrow\uparrow]\rangle\|$	$= 0.024$	$\|\Re\langle[\uparrow\uparrow]\|[\downarrow\uparrow]\rangle\|$	$= 0.026$
$\langle[\uparrow\uparrow\uparrow\uparrow\uparrow\uparrow]\|[\uparrow\uparrow\uparrow\uparrow\uparrow\uparrow]\rangle$	$= 0.45$	$\langle[\uparrow\uparrow\uparrow\uparrow\uparrow\uparrow]\|[\uparrow\uparrow\uparrow\uparrow\uparrow\uparrow]\rangle$	$= 0.0073$
$\|\Re\langle[\uparrow\uparrow\uparrow\uparrow\uparrow\uparrow]\|[\uparrow\uparrow\downarrow\uparrow\uparrow\uparrow]\rangle\|$	$= 0.015$	$\|\Re\langle[\uparrow\uparrow\uparrow\uparrow\uparrow\uparrow]\|[\uparrow\uparrow\downarrow\uparrow\uparrow\uparrow]\rangle\|$	$= 0.0024$
$\|\Re\langle[\uparrow\uparrow\uparrow\uparrow\uparrow\uparrow]\|[\downarrow\uparrow\downarrow\uparrow\downarrow\uparrow]\rangle\|$	$= 7.2 \times 10^{-5}$	$\|\Re\langle[\uparrow\uparrow\uparrow\uparrow\uparrow\uparrow]\|[\downarrow\uparrow\downarrow\uparrow\downarrow\uparrow]\rangle\|$	$= 0.0030$

Table 2: Some elements of the decoherence functional. The quantity $\Delta t = 1$ refers to the time between projections. Entries in the $E_I = 10$ column come from the same initial conditions and coupling strengths as the case presented in Fig 4 from the Schmidt point of view. The $E_I = 1$ column corresponds to Fig 2

Elements of the Decoherence Functional

$\Delta t = 10$

$E_I = 10$			$E_I = 1$		
$\langle[\uparrow\uparrow]\|[\uparrow\uparrow]\rangle$	=	0.82	$\langle[\uparrow\uparrow]\|[\uparrow\uparrow]\rangle$	=	0.38
$\|\Re\langle[\uparrow\uparrow]\|[\downarrow\uparrow]\rangle\|$	=	0.0024	$\|\Re\langle[\uparrow\uparrow]\|[\downarrow\uparrow]\rangle\|$	=	0.069
$\langle[\uparrow\uparrow\uparrow\uparrow\uparrow\uparrow]\|[\uparrow\uparrow\uparrow\uparrow\uparrow\uparrow]\rangle$	=	0.63	$\langle[\uparrow\uparrow\uparrow\uparrow\uparrow\uparrow]\|[\uparrow\uparrow\uparrow\uparrow\uparrow\uparrow]\rangle$	=	0.057
$\|\Re\langle[\uparrow\uparrow\uparrow\uparrow\uparrow\uparrow]\|[\uparrow\uparrow\downarrow\uparrow\uparrow\uparrow]\rangle\|$	=	0.00024	$\|\Re\langle[\uparrow\uparrow\uparrow\uparrow\uparrow\uparrow]\|[\uparrow\uparrow\downarrow\uparrow\uparrow\uparrow]\rangle\|$	=	0.0023
$\|\Re\langle[\uparrow\uparrow\uparrow\uparrow\uparrow\uparrow]\|[\downarrow\uparrow\downarrow\uparrow\downarrow\uparrow]\rangle\|$	=	0.00022	$\|\Re\langle[\uparrow\uparrow\uparrow\uparrow\uparrow\uparrow]\|[\downarrow\uparrow\downarrow\uparrow\downarrow\uparrow]\rangle\|$	=	0.00026

Table 3: Some elements of the decoherence functional. The quantity $\Delta t = 10$ refers to the time between projections. Entries in the $E_I = 10$ column come from the same initial conditions and coupling strengths as the case presented in Fig 4 from the Schmidt point of view. The $E_I = 1$ column corresponds to Fig 2.

The physical differences between the two coupling strengths come out more clearly when one studies the on-diagonal elements, which give the probabilities assigned to the different paths by the decoherence functional. Table 4 show all the on-diagonal elements for the simplest cases. The on-diagonal elements all sum to unity, as required by the decoherence functional theory. At least for the larger two values of Δt, *all* paths have sizable probabilities when $E_I = 1$. That means that if your current state is $|\uparrow\rangle$, for example, you do not know if the your history was $\downarrow\uparrow$ or $\uparrow\uparrow$. In this way that the decoherence functional does indicate the messiness of the the medium coupled case. For the strongly coupled case the probabilities are peaked around the constant spin paths. In the case of $E_I = 1$ and $\Delta t = 0.2$, the probability is also peaked around the constant up path. One could argue that the system has not had time to become messy in this case.

Figure 11 shows the progressive decline of the value of the "constant $\uparrow$" diagonal decoherence functional element as more and more projections are made. The time between projections is fixed at $\Delta t = 0.2$ while the final time is increased. The solid curve is the strongly coupled ($E_I = 10$) case and the dashed curve corresponds to $E_I = 1$. Although from the point of view of the Schmidt paths, the strongly coupled case (Fig 4) exhibits nice spin $\uparrow$ and spin $\downarrow$ paths with relatively *steady* probabilities, the decoherence functional does not directly reveal this behavior. The probability for the constant up path is continually declining, because each projection misses the actual state by a bit. The fluctuations in the weakly coupled case are more wild, so the projection onto $|\uparrow\rangle$ is likely to be further off the mark. This can be seen in the steeper decline of the dashed curve in Fig 11 as compared with the solid ($E_I = 10$) curve.

7.3 The watchdog effect

Figure 12 is the same as Fig 11 except that the time between projection has been reduced to $\Delta t = 0.1$. Now the decline with time is less steep. What we have here is the "watchdog effect" revisited. The projections are so frequent that they are preventing the spin from evolving out of the $|\uparrow\rangle$ state. The appearance of the watchdog effect under these circumstances seems much less attractive, as compared with the discussion in section 5.4. In the present case the projections are not even the result of any real physical interactions. Instead, they are a device introduced by the theorist

$E_I = 10$			$E_I = 1$		
		$\Delta t = 0.2$			
$\langle[\uparrow\uparrow][\uparrow\uparrow]\rangle$	=	0.96	$\langle[\uparrow\uparrow][\uparrow\uparrow]\rangle$	=	0.92
$\langle[\uparrow\downarrow][\uparrow\downarrow]\rangle$	=	0.019	$\langle[\uparrow\downarrow][\uparrow\downarrow]\rangle$	=	0.037
$\langle[\downarrow\uparrow][\downarrow\uparrow]\rangle$	=	0.00041	$\langle[\downarrow\uparrow][\downarrow\uparrow]\rangle$	=	0.0015
$\langle[\downarrow\downarrow][\downarrow\downarrow]\rangle$	=	0.017	$\langle[\downarrow\downarrow][\downarrow\downarrow]\rangle$	=	0.037
Total	=	1.00	Total	=	1.00
		$\Delta t = 1$			
$\langle[\uparrow\uparrow][\uparrow\uparrow]\rangle$	=	0.75	$\langle[\uparrow\uparrow][\uparrow\uparrow]\rangle$	=	0.22
$\langle[\uparrow\downarrow][\uparrow\downarrow]\rangle$	=	0.12	$\langle[\uparrow\downarrow][\uparrow\downarrow]\rangle$	=	0.26
$\langle[\downarrow\uparrow][\downarrow\uparrow]\rangle$	=	0.016	$\langle[\downarrow\uparrow][\downarrow\uparrow]\rangle$	=	0.33
$\langle[\downarrow\downarrow][\downarrow\downarrow]\rangle$	=	0.11	$\langle[\downarrow\downarrow][\downarrow\downarrow]\rangle$	=	0.19
Total	=	1.00	Total	=	1.00
		$\Delta t = 10$			
$\langle[\uparrow\uparrow][\uparrow\uparrow]\rangle$	=	0.82	$\langle[\uparrow\uparrow][\uparrow\uparrow]\rangle$	=	0.38
$\langle[\uparrow\downarrow][\uparrow\downarrow]\rangle$	=	0.062	$\langle[\uparrow\downarrow][\uparrow\downarrow]\rangle$	=	0.14
$\langle[\downarrow\uparrow][\downarrow\uparrow]\rangle$	=	0.0089	$\langle[\downarrow\uparrow][\downarrow\uparrow]\rangle$	=	0.20
$\langle[\downarrow\downarrow][\downarrow\downarrow]\rangle$	=	0.11	$\langle[\downarrow\downarrow][\downarrow\downarrow]\rangle$	=	0.28
Total	=	1.00	Total	=	1.00

Table 4: Sums of on-diagonal elements of the decoherence functional

in order to construct an abstract object (the decoherence functional).

The effect of increasing the frequency of projection (or decreasing the coarse-graining time), as illustrated in Figs 11 and 12, leads to a very peculiar behavior of the probabilities assigned to paths. The solid curve in Fig 11 tells us that if at a time $t = 5$ the spin is up, there is a probability of about 0.6 that it has a history where the spin was exactly up at times separated by $\Delta t = 0.2$. This particular coarse grained history incorporates a multitude of more finely grained histories, where the spin might be doing anything in between the special moments separated by $\Delta t = 0.2$. In particular, the history where the spin is exactly up at instants separated by $\Delta t = 0.1$ is just *one* of the possibilities. However, Fig 12 shows that this single possibility is assigned a larger probability than the entire coarse grained path!

This unusual assignment of probabilities illustrates a problem that a number of people have with the decoherence functional. The concern is that projections involved in constructing the decoherence functional represent interference in the wavefunction evolution on the part of the theorist. There may be cases where this interference is so great as to prevent the real physics from coming to light.

7.4 Defining "sufficiently small"

It turns out that concerns, such as the one raised in the previous subsection, can be resolved by a careful definition of "small" for the off-diagonal elements of the decoherence functional. I will outline the general picture, and then give a particular example.

In any quantum mechanical expression one is at liberty to insert complete sets of states at will, without changing any physical aspect of the expression. One could just as well view this as the insertion of a complete set of projection operators. Of course for a given path projected state, projection operators are inserted singly. However, in any expression involving elements of the decoherence functional, enough off-diagonal decoherence functional elements can be included so that all projections may be viewed as parts of sums over complete sets of projections. In this case the projections can not change the physics in any way. Less complete expressions, which do not involve complete sets of projections, are only generally valid if the net effect of the excluded off-diagonal decoherence functional elements

would have been small. This leads to a natural definition of "small" for the decoherence functional elements, which might be very different from simply comparing them with unity, or with the on-diagonal elements. One can end up requiring that sums over very many off-diagonal decoherence functional elements be small. Under these circumstances even very small individual off-diagonal elements can wind up being "too large".

By way of an example, I return to the "watchdog effect" as illustrated in Figs 11 and 12. The multiple projections represented in these figures will need very many off-diagonal decoherence functional elements to make them "complete". I will simplify things by considering only an elapsed time of $\Delta t = 0.2$. This brings one up to the first projection in Fig 11, and includes the first two projections in Fig 12. I define "$D^{(\tau)}_{\uparrow,\uparrow}$" to be the amplitude squared for finding the spin up at time τ. This is the same as the diagonal decoherence functional element for the "$|\uparrow\rangle$" path at time τ if τ is also the coarse graining time, so there are no intermediate projections. The quantity plotted at $t = 0.2$ on Fig 11 is

$$D^{(0.2)}_{\uparrow,\uparrow} \equiv \langle\psi|\, e^{i\tilde{\Delta}} P_\uparrow e^{-i\tilde{\Delta}} \,|\psi\rangle \tag{33}$$

where

$$\tilde{\Delta} \equiv H_w \times 0.2. \tag{34}$$

By inserting complete sets of projections, this can be rewritten:

$$D^{(0.2)}_{\uparrow,\uparrow} = \langle\psi|\, e^{i\tilde{\Delta}/2}\,(P_\uparrow + P_\downarrow)\, e^{i\tilde{\Delta}/2} P_\uparrow e^{-i\tilde{\Delta}/2}\,(P_\uparrow + P_\downarrow)\, e^{-i\tilde{\Delta}/2} \,|\psi\rangle \tag{35}$$

which is the same as:

$$D^{(0.2)}_{\uparrow,\uparrow} = \langle[\uparrow\uparrow]|[\uparrow\uparrow]\rangle + \langle[\downarrow\uparrow]|[\uparrow\uparrow]\rangle + \langle[\uparrow\uparrow]|[\downarrow\uparrow]\rangle + \langle[\downarrow\uparrow]|[\downarrow\uparrow]\rangle \tag{36}$$

where on the right hand side the time between projection is $\Delta t = 0.1$. The first term on the right side of Eq 36 is the quantity plotted in Fig 12 at $t = 0.2$, namely, the probability assigned to the constant $\uparrow$ path. Table 5 shows the calculated values for each term in Eq 36 (the second two terms in Eq 36 are Hermitian conjugates, and together give twice the real part of one of them). These terms add up, as required by Eq 36. The "peculiar behavior" noted in the previous subsection comes form the fact that the value of $\langle[\uparrow\uparrow]|[\uparrow\uparrow]\rangle$ is larger than the value of $D^{(0.2)}_{\uparrow,\uparrow}$. However,

this behavior is present only to the extent that off-diagonal decoherence functional elements (the second two terms in Eq 36) are non-zero.

Whenever the watchdog effect produces odd behavior, one will always be able to point to off-diagonal decoherence functional elements which are not sufficiently small. Thus one can say that one is not considering "sufficiently decohering" paths. Note that the contribution of the off-diagonal elements is small in Table 5, but that the effect adds up over the long times covered in Figs 11 and 12. In order to write the equivalent of Eq 36 for Figs 11 12, one must include complete sets of projections at many different times, not just at one time as in Eq 35. This results in the appearance of very many off-diagonal decoherence functional elements in the expression. The large "watchdog effect" is not due to any one off-diagonal element being particularly large, but is the result of summing *many* small elements together.

I should note that Eq 36 without the middle two (off-diagonal) terms is an example of the probability sum rules discussed in [28,29,30,31,32]. Quite generally, these sum rules insure that the probabilities assigned coarse grained paths are the sums of the probabilities of individual more finely grained paths. The idea of "decohering paths" is closely linked with the validity of these sum rules. It appears, therefor, that the notion of "small off-diagonal elements" discussed in this subsection is in line with what the authors of [28,29,30,31,32] have in mind.

7.5 Implications

I have shown that the elements of the decoherence functional reflect some of the same properties observed from the Schmidt point of view. However, upon closer inspection one is inclined to reject the "decohering paths" label in both the strong and medium coupled case, because of the violation of natural probability sum rules due to the "watchdog effect".

Table 6 shows the same decoherence functional elements as in Table 5 except that the time between projections is $\Delta t = 10$. One might expect that the watchdog effect can be avoided when the time between projections is sufficiently long. Indeed, Table 6 gives an example where the coarse grained probability ($D^{(20)}_{\uparrow,\uparrow}$) is not lower than that of either fine grained path. However, although the sign of the effect is different, the sum rules are actually violated to roughly the same degree in both Tables 5 and 6,

Elements of the Decoherence Functional
$\Delta t = 0.1$

$E_I = 10$			$E_I = 1$		
$\langle[\uparrow\uparrow]\|[\uparrow\uparrow]\rangle$	=	0.98594	$\langle[\uparrow\uparrow]\|[\uparrow\uparrow]\rangle$	=	0.98025
$2\Re\langle[\uparrow\uparrow]\|[\downarrow\uparrow]\rangle$	=	−0.00309	$2\Re\langle[\uparrow\uparrow]\|[\downarrow\uparrow]\rangle$	=	−0.01915
$\langle[\downarrow\uparrow]\|[\downarrow\uparrow]\rangle$	=	0.00005	$\langle[\downarrow\uparrow]\|[\downarrow\uparrow]\rangle$	=	0.00010
$D^{(0.2)}_{\uparrow,\uparrow}$	=	0.98290	$D^{(0.2)}_{\uparrow,\uparrow}$	=	0.96119

Table 5: The elements of the decoherence functional which appear in Eq [37]. The quantity $\Delta t = 0.1$ refers to the time between projections. Entries in the $E_I = 10$ column come from the same initial conditions and coupling strengths as the case presented in Fig 4 from the Schmidt point of view. The $E_I = 1$ column corresponds to Fig 2.

Elements of the Decoherence Functional
$\Delta t = 10$

$E_I = 10$			$E_I = 1$		
$\langle[\uparrow\uparrow]\|[\uparrow\uparrow]\rangle$	=	0.82064	$\langle[\uparrow\uparrow]\|[\uparrow\uparrow]\rangle$	=	0.38222
$2\Re\langle[\uparrow\uparrow]\|[\downarrow\uparrow]\rangle$	=	0.00485	$2\Re\langle[\uparrow\uparrow]\|[\downarrow\uparrow]\rangle$	=	−0.13851
$\langle[\downarrow\uparrow]\|[\downarrow\uparrow]\rangle$	=	0.00893	$\langle[\downarrow\uparrow]\|[\downarrow\uparrow]\rangle$	=	0.19968
$D^{(20)}_{\uparrow,\uparrow}$	=	0.83442	$D^{(20)}_{\uparrow,\uparrow}$	=	0.44339

Table 6: The elements of the decoherence functional which appear in Eq [37]. The quantity $\Delta t = 10$ refers to the time between projections. Entries in the $E_I = 10$ column come from the same initial conditions and coupling strengths as the case presented in Fig 4 from the Schmidt point of view. The $E_I = 1$ column corresponds to Fig 2.

as indicated by the size of the off-diagonal elements (second row), when compared with $D_{\uparrow,\uparrow}$. If the off diagonal elements in Table 5 are considered too large for the paths to be "decohering", then the same should hold for the large Δt paths in Table 6.

The task of sampling the many possible coarse grainings in time is an enormous one, even for the simple system under study here. I have not undertaken that task for this paper. However, given what I have shown so far, it seems probable that the decoherence functional would not assign "decohering paths" to any of the examples studied in this paper. In each case there are fluctuations present at the level which, at least in the small Δt case resulted in unacceptable violations of the probability sum rules, and which represent interference among individual paths.

Despite the fluctuations, there is quite a bit one can say about the history of the spin system. For example, supposed the spin system were to be used as a one-bit memory device. We have seen (in Figs 4 and 6) that for $E_I = 10$, a spin initially set $|\uparrow\rangle$ would have a probability of roughly 0.8 ± 0.1 to be found in the $|\uparrow\rangle$ state at a later time. This probability can be read directly off the dashed line in the upper plots if the y axis is assumed to run from 0 to 1. It can also be deduced by thinking in term of two Schmidt paths. The most probable path has a probability of roughly 0.8 (solid line, lower plot), and is in a state which fluctuates around $|\uparrow\rangle$ (solid line, upper plot). After the first few units of time, in which the pure $|\uparrow\rangle$ initial state degrades (Fig 4), the fluctuations appear to be stable, even after long times have elapsed (Fig 6).

There is no doubt that this system makes a lousy memory device. However, even in this primitive form, one can see that it makes a much better memory device than the system with medium coupling (Fig 2). The key difference is that in the strongly coupled case the fluctuations are relatively small and very stable. In order to improve the device, one would want to reduce the size of the fluctuations, and cause them to become stabilized much closer to the pure $|\uparrow\rangle$ initial state. None the less, one could not expect the fluctuations to completely disappear in any realistic situation.

The necessary improvements in this "memory device" can easily be realized by simply increasing E_I. Figure 13 shows the same setup as Fig 4 with E_I increased to 100. Now all fluctuations are down to roughly the 1% level. The future evolution of the system initially set "$|\uparrow\rangle$" is dominated by a single Schmidt path whose state is very close to "$|\uparrow\rangle$" at all times.

A subsequent measurement of the spin has around a 99% probability of turning out "correctly".

I have also performed the decoherence functional analysis on the $E_I = 100$ example. Not surprisingly, the system is much closer to exhibiting "decohering paths". The ratio of $2\Re\langle[\uparrow\uparrow]|[\downarrow\uparrow]\rangle$ to $\langle[\uparrow\uparrow]|[\uparrow\uparrow]\rangle$, for $\Delta t = 0.1$ is -0.00028 as compared with -0.0031 (from Table 5) for $E_I = 10$. That means the sum rule (Eq 36 without the middle two terms) is violated to that much less of a degree. After an elapsed time of five units, the ratio of the probabilities for the constant $|\uparrow\rangle$ paths, comparing $\Delta t = 0.1$ with $\Delta t = 0.2$ is 1.0033 for $E_I = 100$, as compared with 1.14 for $E_I = 10$ (from Figs 11 and 12). This indicates a smaller "watchdog effect".

However, one only has to consider long enough times to observe the sum rules violated to any given degree. One just has to wait longer when $E_I = 100$. This is because the presence of fluctuations, no matter how small, steadily reduced the extent to which paths "decohere". By contrast, as long as these fluctuations are stable, they do not systematically decrease the reliability of the system as a memory device as time progresses. This perspective is easily available from the Schmidt analysis.

The discussion here illustrates a way in which the decoherence functional and the Schmidt paths appear to emphasize different physical properties of the system under consideration. In section 7.2 I showed ways in which the two approaches reflected similar aspects of the physics. It remains to be seen whether it is the similarities or the differences which come out most strongly when these ideas are applied in other situations.

8 Comparison with other work

Other authors have also studied two state systems coupled to an environment. In particular such systems appear in some of the pioneering papers on quantum decoherence [3,9]. The main way the calculations presented here differ from previous work is that here exact (to machine precision) solutions are provided for a much more complex system then most of those which were solved exactly before. The work also represents the first time a side-by-side comparison of the decoherence functional and the Schmidt paths has been made. In most previous work, the cases which were solved exactly were very simple. Some cases involved a Hamiltonian which was

(or became) exactly separable. In other cases the pointer basis states were exact eigenstates of the total Hamiltonian. These simplifications made it easy for correlations to be discussed, since they were exactly preserved as time evolved. (Another complex example which is solved exactly is given by Unruh and Zurek [7].)

More complex examples have been studied, but various approximations were used. One thing the work here shows clearly is how there are many ways the Schmidt states can deviate from a simple pointer basis. In some cases the deviations are large, while in other cases the deviations amount to small, stable fluctuations. (Presumably the latter fluctuations are present at some level in *any* realistic example.) I believe that the previous work was sufficiently simplified as to not distinguish among these different possibilities. For example, the *timescale* of these deviations alone is not enough to distinguish between the two cases.

The model studied here is very close in spirit to Zurek's model in [3], but it is less idealized. Although plots appear in [3] of off-diagonal density matrix elements which are small, but not precisely zero, the plots are for the case where the on-diagonal elements are degenerate. In this case the off-diagonal elements would be equally small in *any* basis, and the interactions being studied do not help choose a pointer basis. It is actually the correlations between the spin and the "apparatus atom" which determine the pointer basis, and these are preserved exactly, because the interactions have been turned off (this point is discussed further in [35]).

I should stress, however, that I am not calling into question, or even adding to the major advances made by Zurek [3] and by Joos and Zeh [9] in in identifying the mechanisms which cause decoherence, and their important role in quantum physics. What I am doing in this paper is trying out different ways of viewing these mechanisms in action, on a system with a slightly more realistic degree of complexity.

9 Conclusions

I have investigated the decohering properties of a simple toy system from a number of points of view. One goal was to determine to what extent the interactions with the environment defined a "pointer basis" whose quantum coherence was not destroyed by the interactions.

In the "Schmidt Paths" point of view, the system was studied by following the evolution of the eigenstates of the reduced density matrix. Depending on the coupling strength, there was either: 1) A constant pointer basis (strong coupling), 2) A simply oscillating pointer basis (weak coupling), or 3) Noisy behavior, with no pointer basis (medium coupling). I also illustrated how the standard approach of looking at the off-diagonal elements of the density matrix would not have clearly revealed this behavior.

The situation was not as simple when the density matrix had nearly degenerate eigenvalues. Due to the simplicity of the model, it is not clear if this just represents correct high entropy physics, or if the Schmidt decomposition is not as useful under these circumstances.

The decoherence functional approach was also used, and applied to both the strong and medium coupling regimes This formalism provides a way to determine the extent to which probabilities can be assigned to separate paths or histories of a quantum system. The different physics of the strong and medium couplings was apparent in the decoherence functional elements calculated. However, I argued that care must be taken in defining "sufficiently decohering" paths. By one reasonable definition, it appears that none of the cases considered in this paper could be assigned decohering histories. This was because fluctuations caused too much interference among the different paths. Still, I showed that there was a less stringent sense in which histories could be discussed. I raised the question whether the decoherence functional might be too strict a way of discussing histories for some applications.

The work presented here serves to illustrate two different ways of thinking about quantum decoherence. These approaches operate in very different ways, and to some extent emphasize different aspects of the physics. Of course the way these approaches must prove themselves is by providing new insights which contribute to the progress of physics. How, in the end, the Schmidt paths and the decoherence functional measure up to this standard still remains to be seen.

10 Acknowledgements

I am greatly indebted to Wojtek Zurek for valuable ongoing discussions on this subject. I would also like to thank Fay Dowker, Johnathan Halliwell,

Seth Lloyd, and Richard Matzner for very helpful conversations. This work was supported in part by the DOE and the NASA (grant NAGW-1340) at Fermilab.

A The Schmidt Decomposition

A.1 Proof

Here is a brief proof that the Schmidt decomposition may always be performed: Consider a state $|\psi\rangle$ in a vector space which we choose to regard as a direct product space. Let $\{|i\rangle_1\}$ and $\{|j\rangle_2\}$ each be some orthonormal basis in the corresponding subspace. There always exist α_{ij}'s such that

$$|\psi\rangle = \sum_{ij} \alpha_{ij}|i\rangle_1|j\rangle_2. \tag{37}$$

Furthermore, one can define

$$|\tilde{i}\rangle_2 \equiv \sum_j \alpha_{ij}|j\rangle_2 \tag{38}$$

So that one can always write

$$|\psi\rangle = \sum_i |i\rangle_1|\tilde{i}\rangle_2. \tag{39}$$

In general, the $|\tilde{i}\rangle_2$'s will not be orthogonal or normalized.

Now consider the special case were the $\{|i\rangle_1\}$ are the (normalized) eigenstates of ρ_1 ($\equiv \mathbf{tr}_2(|\psi\rangle\langle\psi|) = \sum_{ijk} \alpha^*_{ij}\alpha_{kj}|i\rangle_1\,{}_1\langle k|$), call them $\{|i\rangle_1^S\}$. In this case the $\{|\tilde{i}\rangle_2\}$ *must* be orthogonal, because we must have

$${}^S_1\langle i|\rho_1|j\rangle^S_1 = {}^S_1\langle i|\left(\sum_{k,l}|k\rangle^S_1\,{}_2\langle\tilde{k}|\tilde{l}\rangle_2\,{}^S_1\langle l|\right)|j\rangle^S_1 = {}_2\langle\tilde{i}|\tilde{j}\rangle_2 \propto \delta_{ij} \tag{40}$$

One can then see that the $|\tilde{i}\rangle_*$'s must be eigenstates of ρ_2 :

$$\rho_2 \equiv \mathbf{tr}_1(|\psi\rangle\langle\psi|) = \sum_i |\tilde{i}\rangle_2\,{}_2\langle\tilde{i}|. \tag{41}$$

Finally, one notes that the non-zero eigenvalues of both ρ_1 and ρ_2 are both given by $p_i = {}_2\langle\tilde{i}|\tilde{i}\rangle_2$, and one can construct the normalized states:

$$|i\rangle^S_2 \equiv (p_i)^{-1/2}|\tilde{i}\rangle_2. \tag{42}$$

Equation 39 then becomes

$$|\psi\rangle = \sum_i \sqrt{p_i}\,|i\rangle^S_1\,|i\rangle^S_2\,, \tag{43}$$

which is the quoted result.

A.2 Remarks

Here is a remark which often helps people develop some intuition about the Schmidt decomposition: If one is given a particular vector in a vector space, and is allowed complete freedom to choose a basis, one can always choose a basis in which the expansion of the particular vector has but one term. One simply chooses the first basis vector proportional to the state in question. To get a complete basis, one then constructs an orthonormal set around that first basis vector (using the Gram-Schmidt orthogonalization procedure). If one does not have *complete* freedom to choose a basis, but is allowed to choose any bases within two pre-determined subspaces, then it should not be surprising that in general one can not get down to a single term in the expansion. However, one should be able reduce the number of terms, since there is some remaining flexibility, and that is what the Schmidt form does. Note that the number of terms in Eq (43) is equal to the *minimum* of the two subspace sizes, rather than the *product* of the two sizes which would arise in a typical expansion.

B Computational Methods

The computational methods employed in this work are straightforward. The total Hilbert space has a size of $2n_1$, where n_1 is the size of the environment subspace. I start by considering an orthonormal set $\{|i\rangle_w | i = 1, 2n_1\}$ (the "working basis"), which spans the whole space. This set may be viewed as a direct product of two sets of vectors, $\{|\uparrow\rangle_2, |\downarrow\rangle_2\}$, and $\{|j\rangle_1 | j = 1, n_1\}$, each of which spans one of the two subspaces. The direct product form for each $|i\rangle_w$ can be realized by writing

$$|i\rangle_w = \begin{cases} |\uparrow\rangle \otimes |(i+1)/2\rangle_1 & i = \text{odd} \\ |\downarrow\rangle \otimes |(i)/2\rangle_1 & i = \text{even} \end{cases} . \tag{44}$$

In this way a working basis is defined in each of the subsystems as well. Any state of the system can be represented by a set of $2n_1$ complex numbers, α_i, normalized to $\sum_i \alpha_i^* \alpha_i = 1$, giving the expansion coefficients of the state in the working basis. These number can be equivalently labeled $\alpha_{\uparrow,(i+1)/2}$ or $\alpha_{\downarrow,(i)/2}$ according to Eq 44. Likewise, any operator can be represent by a $2n_1 \times 2n_1$ array of numbers giving all the matrix elements of the operator in the working basis.

In order to do a calculation, first the expansion coefficients of the initial state in the working basis are calculated. Then the array corresponding to the total Hamiltonian is constructed, and diagonalized (using a packaged subroutine from IMSL). One then has a spectrum of eigenvalues $\{E_i\}$, and a unitary operator $\hat{U}$ for transforming in and out of the eigenbasis. Using $\hat{U}$, I calculate the expansion coefficients of the state in the eigenbasis of the Hamiltonian. Then time evolution is reduced to evaluating a new phase, e^{-iE_it}, for each of the energy eigenbasis expansion coefficients.

At any time $\hat{U}^\dagger$ can be used to return to the expansion coefficients in the working basis. In this basis, it is easy to construct the matrix elements of ρ_2, or any other quantity of interest. For example

$$\langle\uparrow|\,\rho_2\,|\downarrow\rangle = \sum_{j=1}^{n_1} \alpha^*_{\uparrow,j}\alpha_{\downarrow,j}. \tag{45}$$

With all the elements of ρ_2 in hand, one can then diagonalize it, and examine the eigenvalues and eigenvectors, leading to the Schmidt paths. Likewise, the projections needed to construct the decoherence functional are easy to perform.

C Other numerical issues

C.1 The size of the environment

All the cases discussed in the main part of the paper had $n_1 = 12$. I have studied the system for a variety of different n_1's. The value 12 was chosen because it was large enough for the environment to play the desired role, but not much larger, so the computations could run as rapidly as possible. As an illustration, Figures 14 and 15 show the large E_I case for different values of n_1. The values of E_I are chosen so that $E_I \cdot \sqrt{n_1} = 10 \cdot \sqrt{12}$. This keeps the size of a typical energy eigenvalue constant, and makes comparison more convenient. (See Fig 4 for the $E_I = 10, n_1 = 12$ case.)

C.2 Tests of the code

All calculations were performed with double precision complex numbers on a VAX computer. In general, there should not be a problem in accurately

evaluating the time dependent phases of the energy eigenstates for the time ranges considered. In any case, one does not expect numerical errors to build up in time in this sort of calculation. The state of the world at each time is calculated directly by shifting the phases of the initial state as expanded in the energy eigenstates. There is no dependence on the state at intermediate times.

Perhaps, one could be concerned that the correct physics depends on the realization of precise relationships among the energy eigenstates. One example of this is the $E_I = 0$ case, where the simple evolution of system 2 depends on the relationship $\lambda_i - \lambda_j = E_2$ holding among pairs of energy eigenvalues of the "world". Figure 16 shows the results for a $E_I = 0$ case observed at late times. The fact that the expected simple sinusoidal evolution is realized indicates that the program is working properly. Note the large size the environment ($n_1 = 50$). Half of the 100 energy eigenstates have an appreciable overlap with the initial state, so the simple evolution depicted in Fig 16 shows that the special relationships among all these states are being correctly accounted for. The choice of $E_2 = \pi$ was made so that the phase of the oscillations can also be easily checked to be correct by inspecting Fig 16. Note also that the entropy remains "exactly" zero, as it should.

Another confirmation of the code comes from the manifestation of the correct relationships among the numbers in Tables 4, 5, and 6. In the first case, the elements sum to unity, and in the later two cases, Eq 36 is obeyed. (The tables actually include some rounding error, since not all digits are presented. The code realizes the required relationships to much higher precision.)

Each calculation uses a particular random number seed to generate the parts of the Hamiltonian and of the initial state designated as "random". The seed was changed from time to time, and it does not appear that any results reported here represent atypical realizations. This issue was not investigated systematically, however.

References

[1] H. D. Zeh. *Found. of Phys.*, 3:109, 1973.

[2] W. Zurek. *Phys. Rev. D*, 24:1516, 1981.

[3] W.H. Zurek. *Phys. Rev. D*, 26:1862, 1982.

[4] W.H. Zurek. Pointer basis and inhibition of quantum tunneling by environment-induced superselection. In *Proc. Int. Symp. Foundations of Quantum Mechanics, Tokyo*, page 181, 1983.

[5] A. O. Caldeira and A. J. Leggett. *Physica*, 121A:587, 1983.

[6] W.H. Zurek. Reduction of the wave packet: How long does it take? In *Frontiers of nonequilibrium statistical physics*. Plenum, 1986.

[7] W. Unruh and W. Zurek. *Phys. Rev. D*, 40:1071, 1989.

[8] R. Omnès. Some progress in measurement thoery: The logical interpretation of quantum mechanics. In W. H. Zurek, editor, *Complexity, Entropy and the Physics of Information*. Addison Wesley, 1990.

[9] E. Joos and H.D. Zeh. *Zeit. Phys.*, B59:223, 1985.

[10] S. Hawking. *Phys. Lett.*, 115B:295, 1982.

[11] A. Starobinski. *Phys. Lett.*, 117B:175, 1982.

[12] A. Guth and S.-Y. Pi. *Phys. Rev. Lett.*, 49:1110, 1982.

[13] J. Bardeen, P. Steinhardt, and M. Turner. *Phys. Rev. D*, 28:679, 1983.

[14] R. Brandenberger, R. Laflame, and M. Mijić. Classical perturbations from decoherence of quantum fluctuations in the inflationary universe. Brown preprint BROWN-HET-741, 1990.

[15] J. J. Halliwell. *Phys. Rev. D*, 39:2912, 1989.

[16] S. W. Hawking, D. N. Page, and C. N. Pope. *Nucl. Phys.*, B170:283, 1980.

[17] S. W. Hawking. In H. A. Brück, G. V. Coyne, and M.S Longair, editors, *Study Week on Cosmology and Fundamental Sciences*. Pontificia Academia Scientiarum Cittá Del Vaticano, 1982.

[18] A. Strominger. *Phys. Rev. Lett.*, 52:1733, 1984.

[19] D. Gross. *Nucl. Phys.*, B236:349, 1984.

[20] S. W. Hawking. *Phys. Lett.*, 195B:337, 1987.

[21] G. V. Lavrelashvili, V. A. Rubakov, and P. G. Tinyakov. *JETP Lett.*, 46:167, 1987.

[22] S. W. Hawking. *Phys. Rev. D*, 37:904, 1988.

[23] S. Giddings and A. Strominger. *Nucl. Phys.*, B306:890, 1988.

[24] S. Coleman. *Nucl. Phys.*, B308:867, 1988.

[25] A. J. Leggett et al. *Rev. Mod. Phys.*, 59:1, 1987.

[26] A. O. Caldeira and A. Leggett. *Ann. Phys.*, 143, 1983.

[27] C.D. Tesche. *Ann. N. Y. Acad. Sci*, 480, 1986.

[28] R. Griffiths. *J. Stat. Phys.*, 36:219, 1984.

[29] R. Omnès. *J. Stat. Phys.*, 53:893, 1988.

[30] R. Omnès. *J. Stat. Phys.*, 53:933, 1988.

[31] R. Omnès. *J. Stat. Phys.*, 53:957, 1988.

[32] M. Gell-Mann and J. B. Hartle. Quantum mechanics in the light of quantum cosmology. In W. H. Zurek, editor, *Complexity, Entropy and the Physics of Information.* Addison Wesley, 1990.

[33] J.B. Hartle. The quantum mechanics of cosmology. Lectures presented at the Jerusalem winter school on Quantum Cosmology and Baby Universes, 1990.

[34] O. Kübler and H. D. Zeh. *Ann. Phys.*, page 405, 1973.

[35] A. Albrecht. Identifying decohering paths in closed quantum systems. FERMILAB-Pub-90/128-A, see also [39], 1990.

[36] E. Schmidt. *Math. Annalen*, 63:433, 1907.

[37] H. D. Zeh. Quantum measurements and entropy. In W. H. Zurek, editor, *Complexity, Entropy and the Physics of Information.* Addison Wesley, 1990.

[38] A.O. Barvinsky and A.Yu. Kamenshchik. *Class. and Quantum Gravity*, 7:2285, 1990.

[39] A. Albrecht. Revised version of [35], in preperation, 1991.

[40] Misra B and E. C. G. Sudarshan. *J. Math. Phys.*, 18:756, 1977.

[41] K. Kraus. *Found. of Phys.*, 11:547, 1981.

[42] Y. Aharonov and M. Vardi. *Phys. Rev. D*, 21:2235, 1980.

[43] A. Peres. *Am. J. Phys.*, 48:931, 1980.

Figure Captions

Figure 1: Weak coupling ($H_1 = H_2 = 1$, $H_I = 0.3$), with a $|\uparrow\rangle_2 \otimes |\text{random}\rangle_1$ initial state. (a): Solid line is $\langle \hat{J} \rangle$ for an eignestate of ρ_2. Dashed line is ${}_w\langle\psi|\hat{J} \otimes I_1|\psi\rangle_w$. (b): Dashed line is the entropy, solid line is the largest eigenvalue of ρ_2. The size of the environment, $n_1 = 12$

Figure 2: Medium coupling ($H_1 = H_2 = 1$, $H_I = 1$), with a $|\uparrow\rangle_2 \otimes |\text{random}\rangle_1$ initial state. (a): Solid line is $\langle \hat{J} \rangle$ for an eignestate of ρ_2. Dashed line is ${}_w\langle\psi|\hat{J} \otimes I_1|\psi\rangle_w$. (b): Dashed line is the entropy, solid line is the largest eigenvalue of ρ_2. The size of the environment, $n_1 = 12$

Figure 3: Stronger coupling ($H_1 = H_2 = 1$, $H_I = 3$), with a $|\uparrow\rangle_2 \otimes |\text{random}\rangle_1$ initial state. (a): Solid line is $\langle \hat{J} \rangle$ for an eignestate of ρ_2. Dashed line is ${}_w\langle\psi|\hat{J} \otimes I_1|\psi\rangle_w$. (b): Dashed line is the entropy, solid line is the largest eigenvalue of ρ_2. The size of the environment, $n_1 = 12$

Figure 4: Strong coupling ($H_1 = H_2 = 1$, $H_I = 10$), with a $|\uparrow\rangle_2 \otimes |\text{random}\rangle_1$ initial state. (a): Solid line is $\langle \hat{J} \rangle$ for an eignestate of ρ_2. Dashed line is ${}_w\langle\psi|\hat{J} \otimes I_1|\psi\rangle_w$. (b): Dashed line is the entropy, solid line is the largest eigenvalue of ρ_2. The size of the environment, $n_1 = 12$

Figure 5: Values of $|\langle\uparrow|\rho_2|\downarrow\rangle|$ as a function of time. The dashed curve corresponds to the stongly coupled case shown in Fig 4, and the solid curve is the $H_I = 1$ case in Fig 2.

Figure 6: Strong coupling ($H_1 = H_2 = 1$, $H_I = 10$), with a $|\uparrow\rangle_2 \otimes |\text{random}\rangle_1$ initial state. (a): Solid line is $\langle \hat{J} \rangle$ for an eignestate of ρ_2. Dashed line is ${}_w\langle\psi|\hat{J} \otimes I_1|\psi\rangle_w$. (b): Dashed line is the entropy, solid line is the largest eigenvalue of ρ_2. The size of the environment, $n_1 = 12$

Figure 7: Strong coupling ($H_1 = H_2 = 1$, $H_I = 10$), with a random initial state. (a): Solid line is $\langle \hat{J} \rangle$ for an eignestate of ρ_2. Dashed line is ${}_w\langle\psi|\hat{J} \otimes I_1|\psi\rangle_w$. (b): Dashed line is the entropy, solid line is the largest eigenvalue of ρ_2. The size of the environment, $n_1 = 12$

Figure 8: Ultra-strong coupling ($H_1 = H_2 = 0.001$, $H_I = 10000$), with a random initial state. (a): Solid line is $\langle \hat{J} \rangle$ for an eignestate of ρ_2. Dashed line is ${}_w\langle\psi|\hat{J} \otimes I_1|\psi\rangle_w$. (b): Dashed line is the entropy, solid line is the largest eigenvalue of ρ_2. Dashed line is ${}_w\langle\psi|\hat{J} \otimes I_1|\psi\rangle_w$. (b): Dashed line is the entropy, solid line is the largest eigenvalue of ρ_2. The size of the environment, $n_1 = 12$

Figure 9: Weak coupling ($H_1 = H_2 = 1$, $H_I = 0.3$), with a random initial state. (a): Solid line is $\langle \hat{J} \rangle$ for an eignestate of ρ_2. Dashed line is ${}_w\langle\psi|\hat{J} \otimes I_1|\psi\rangle_w$. (b): Dashed line is the entropy, solid line is the largest eigenvalue of ρ_2. The size of the environment, $n_1 = 12$

Figure 10: Weak coupling ($H_1 = H_2 = 1$, $H_I = 0.3$), with a $|\uparrow\rangle_2 \otimes |\text{random}\rangle_1$ initial state. (a): Solid line is $\langle \hat{J} \rangle$ for an eignestate of ρ_2. Dashed line is ${}_w\langle\psi|\hat{J} \otimes I_1|\psi\rangle_w$. (b): Dashed line is the entropy, solid line is the largest eigenvalue of ρ_2. The size of the environment, $n_1 = 12$

Figure 11: The value of the probability assigned by the decoherence functional to the constant $\uparrow$ path as a function of final time. The spacing between projections remains a constant $\Delta t = 0.2$. The solid line is for $H_I = 10$ and the dashed line is for $H_I = 1$.

Figure 12: The value of the probability assigned by the decoherence functional to the constant $\uparrow$ path as a function of final time. The spacing between projections remains a constant $\Delta t = 0.05$. The solid line is for $H_I = 10$ and the dashed line is for $H_I = 1$.

Figure 13: Very strong coupling ($H_1 = H_2 = 1$, $H_I = 100$), with a $|\uparrow\rangle_2 \otimes |\text{random}\rangle_1$ initial state. (a): Solid line is $\langle \hat{J} \rangle$ for an eignestate of ρ_2. Dashed line (barely distinguishable from the solid line) is ${}_w\langle\psi|\hat{J} \otimes I_1|\psi\rangle_w$. (b): Dashed line is the entropy, solid line is the largest eigenvalue of ρ_2. The solid line is from numbers recorded to only two decmial places. This fact influences the detailed shape of the curve. The size of the environment, $n_1 = 50$

Figure 14: Strong coupling, large environment ($H_1 = H_2 = 1$, $H_I = 4.9$), with a $|\uparrow\rangle_2 \otimes |\text{random}\rangle_1$ initial state. (a): Solid line is $\langle \hat{J} \rangle$ for an eignestate of ρ_2. Dashed line is ${}_w\langle\psi|\hat{J} \otimes I_1|\psi\rangle_w$. (b): Dashed line is the entropy, solid line is the largest eigenvalue of ρ_2. The size of the environment, $n_1 = 50$

Figure 15: Strong coupling, small environment ($H_1 = H_2 = 1$, $H_I = 15.5$), with a $|\uparrow\rangle_2 \otimes |\text{random}\rangle_1$ initial state. (a): Solid line is $\langle \hat{J} \rangle$ for an eignestate of ρ_2. Dashed line is ${}_w\langle\psi|\hat{J} \otimes I_1|\psi\rangle_w$. (b): Dashed line is the entropy, solid line is the largest eigenvalue of ρ_2. The size of the environment, $n_1 = 5$

Figure 16: A test calculation with zero coupling and a large environment ($H_1 = 1, H_2 = \pi$, $H_I = 0$), with a $|\uparrow\rangle_2 \otimes |\text{random}\rangle_1$ initial state. (a): Solid line is $\langle \hat{J} \rangle$ for an eignestate of ρ_2. Dashed line is ${}_w\langle\psi|\hat{J} \otimes I_1|\psi\rangle_w$. These two curves are indistinguishable. (b): Dashed line is the entropy, solid line is the largest eigenvalue of ρ_2. The size of the environment, $n_1 = 50$

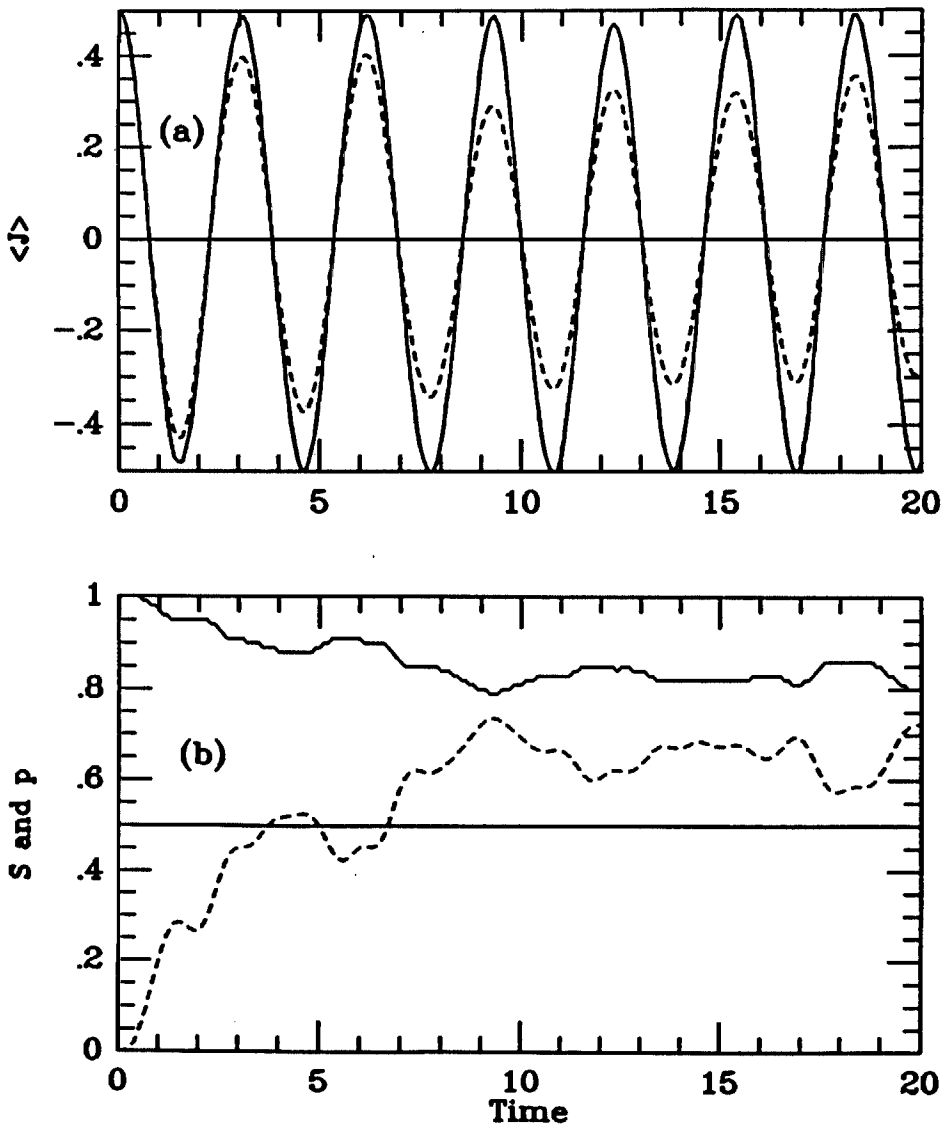
(a)
<J>
.4
.2
0
-.2
-.4
0
5
10
15
20
(b)
S and p
1
.8
.6
.4
.2
0
Time

Fig 1

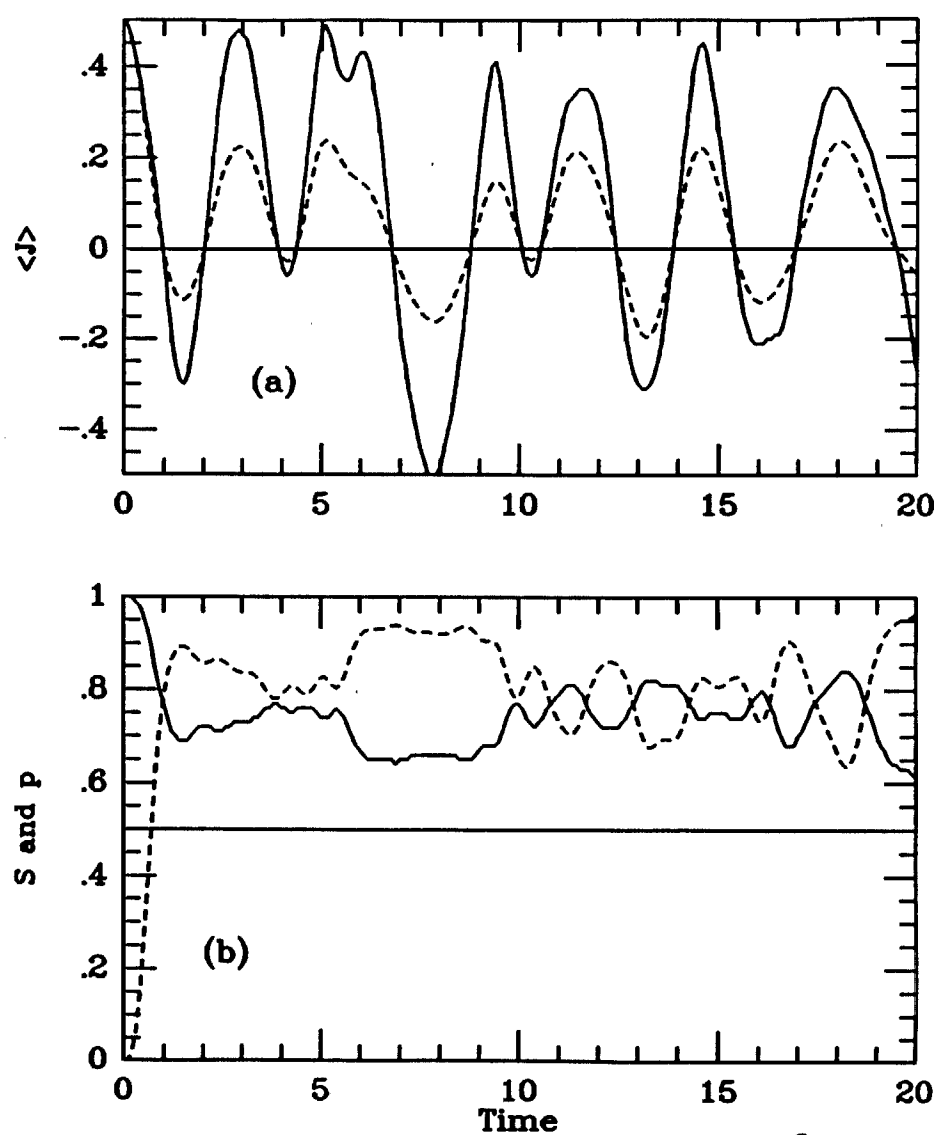
(a)
<J>
.4
.2
0
-.2
-.4
0
5
10
15
20
(b)
S and p
1
.8
.6
.4
.2
0
Time

Fig 2

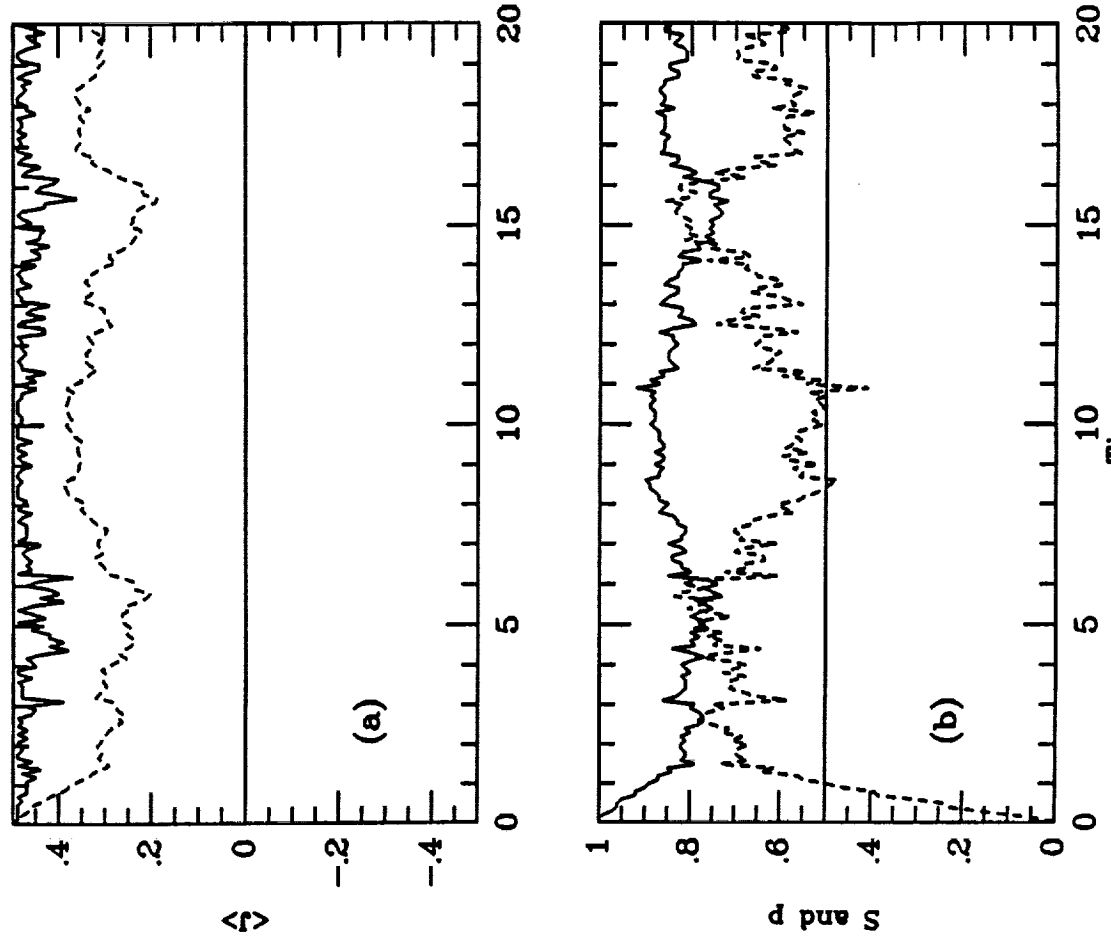
(a)
(b)
<j>
S and p
Time
0
5
10
15
20
.4
.2
0
-.2
-.4
1
.8
.6
.4
.2

Fig 4

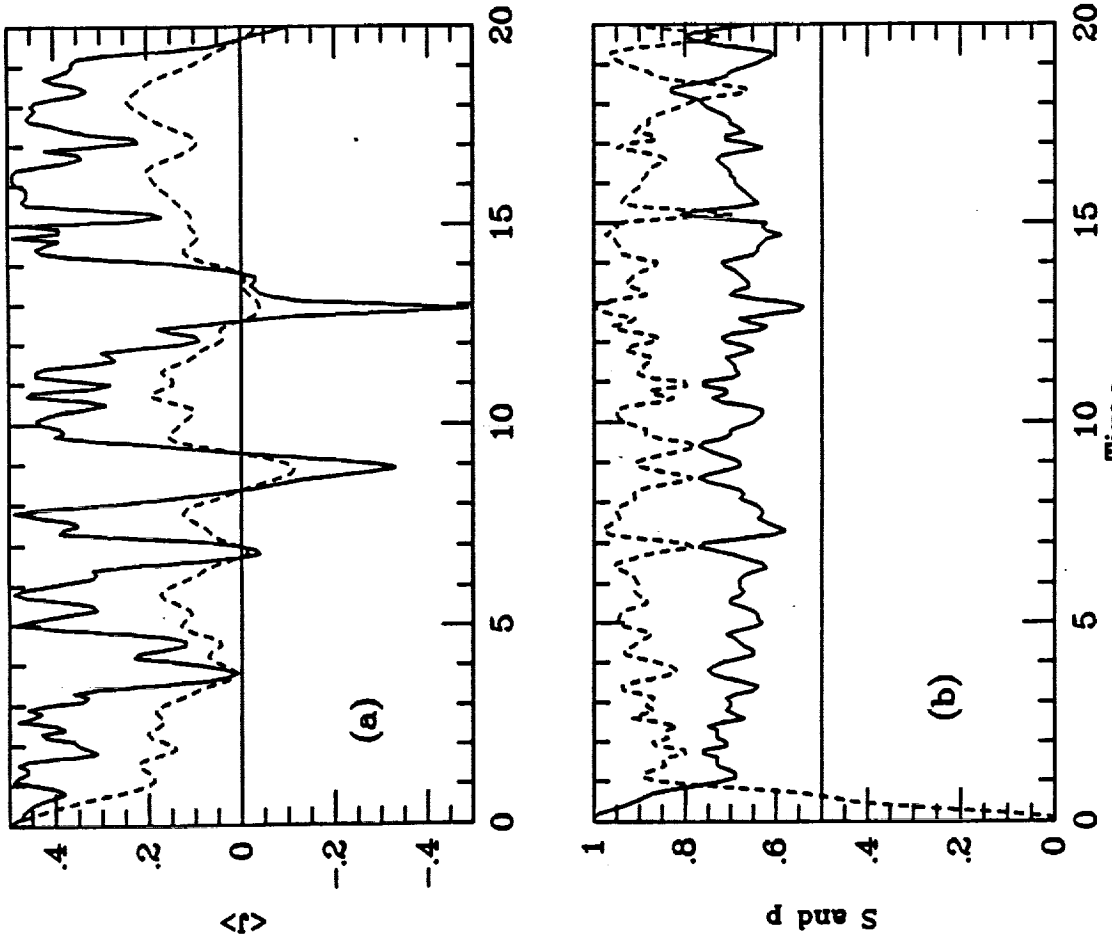
(a)
(b)
<j>
S and p
Time
0
5
10
15
20
.4
.2
0
-.2
-.4
1
.8
.6
.4
.2

Fig 3

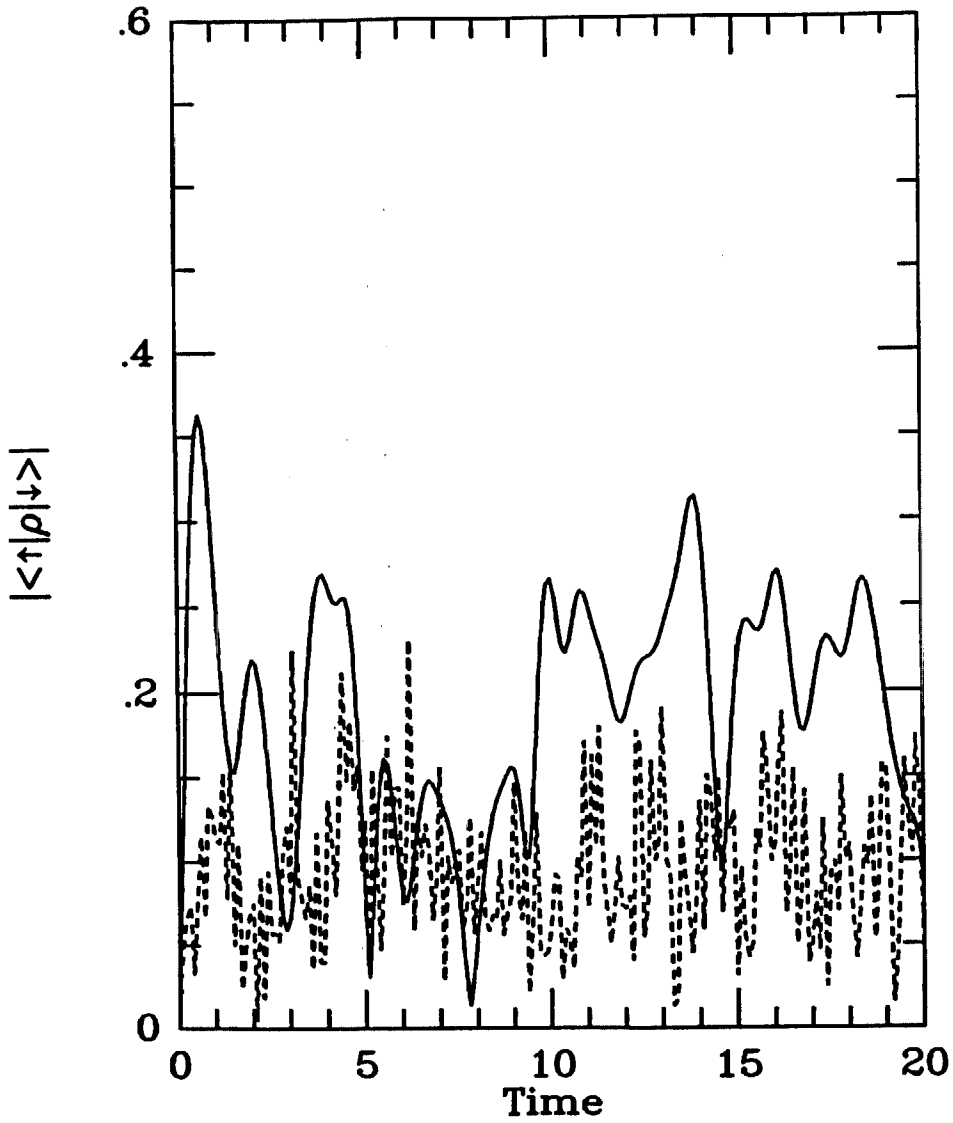
.6
.4
.2
0
|<↑|ρ|↓>|
0
5
10
15
20
Time

Fig 5

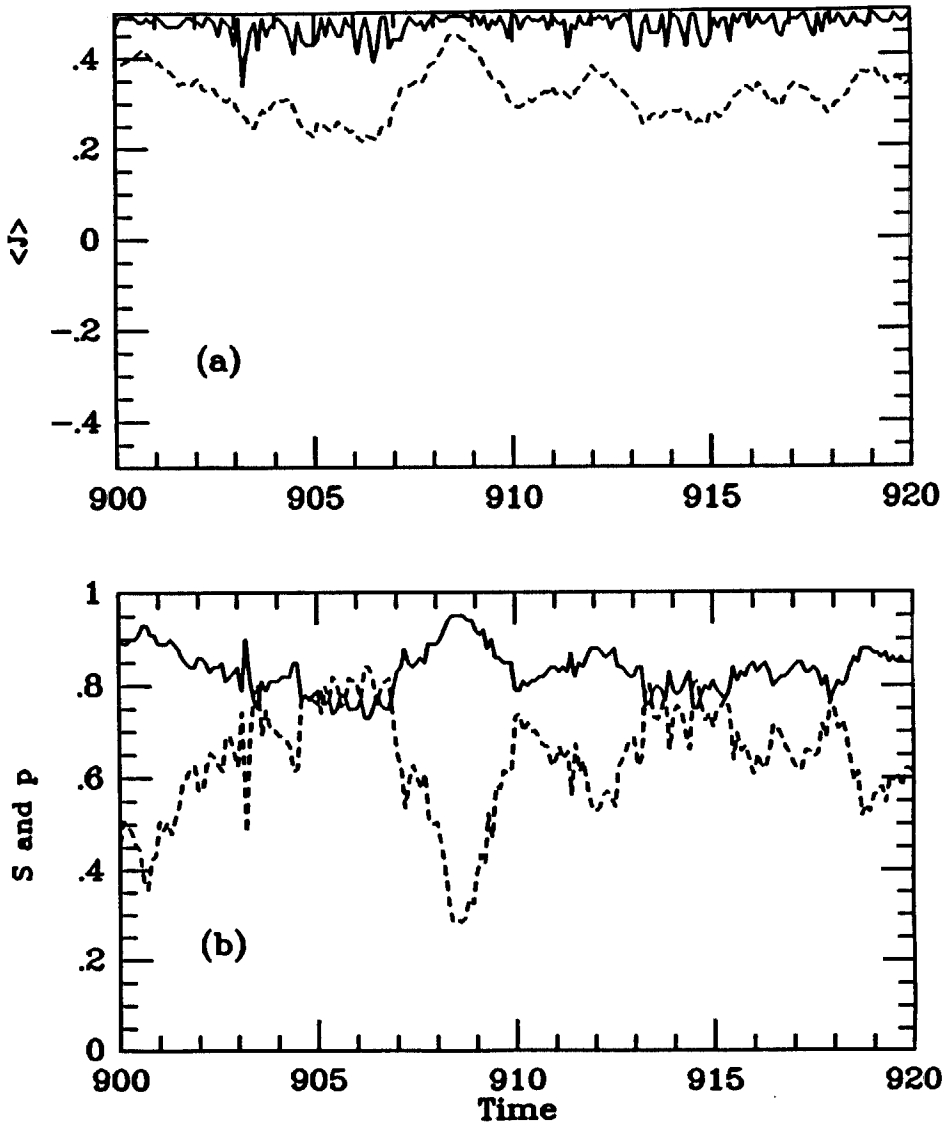
.4
.2
0
-.2
-.4
<J>
(a)
900
905
910
915
920
1
.8
.6
.4
.2
0
S and p
(b)
900
905
910
915
920
Time

Fig 6

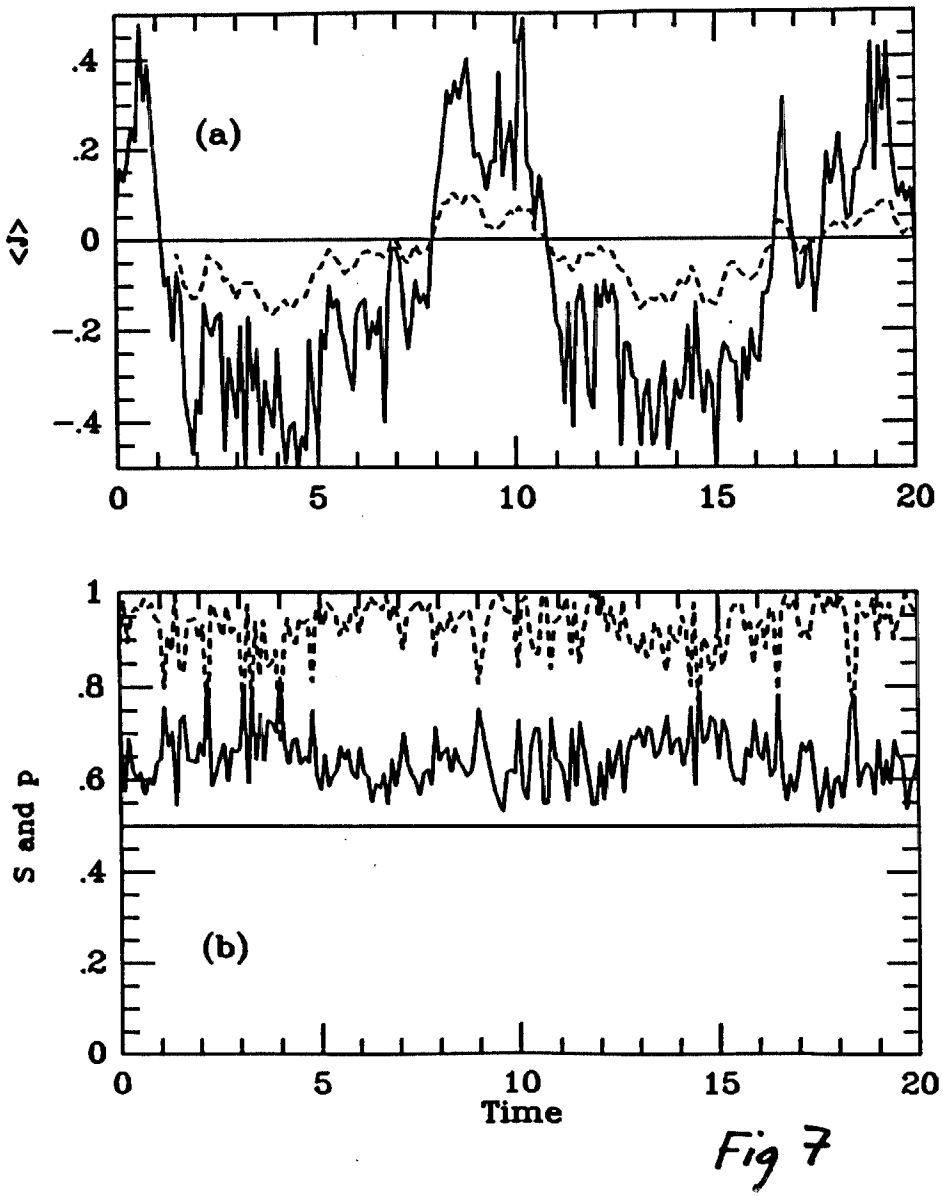
(a)
<J>
.4
.2
0
-.2
-.4
0
5
10
15
20
(b)
S and p
1
.8
.6
.4
.2
0
Time

Fig 7

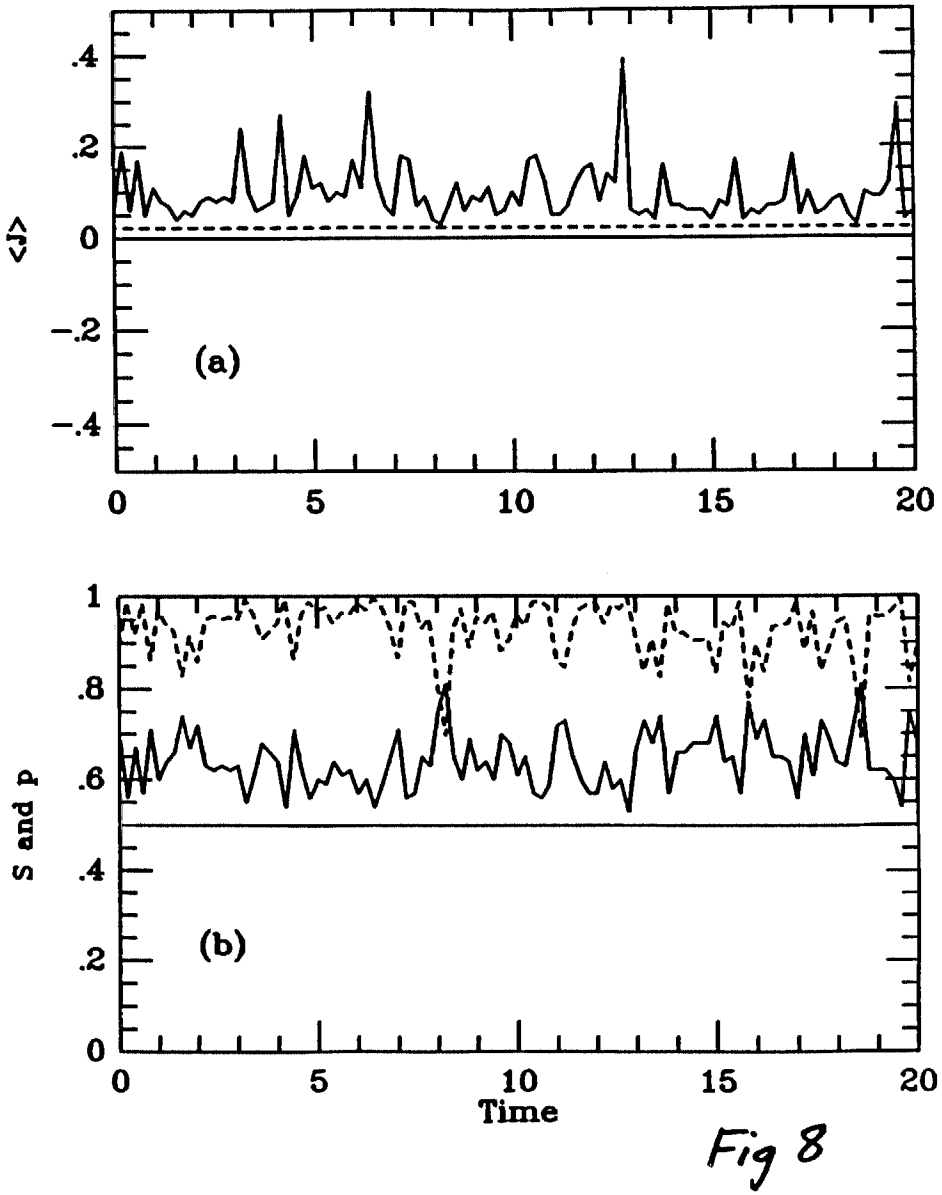
(a)
<J>
.4
.2
0
-.2
-.4
0
5
10
15
20
(b)
S and p
1
.8
.6
.4
.2
0
Time

Fig 8

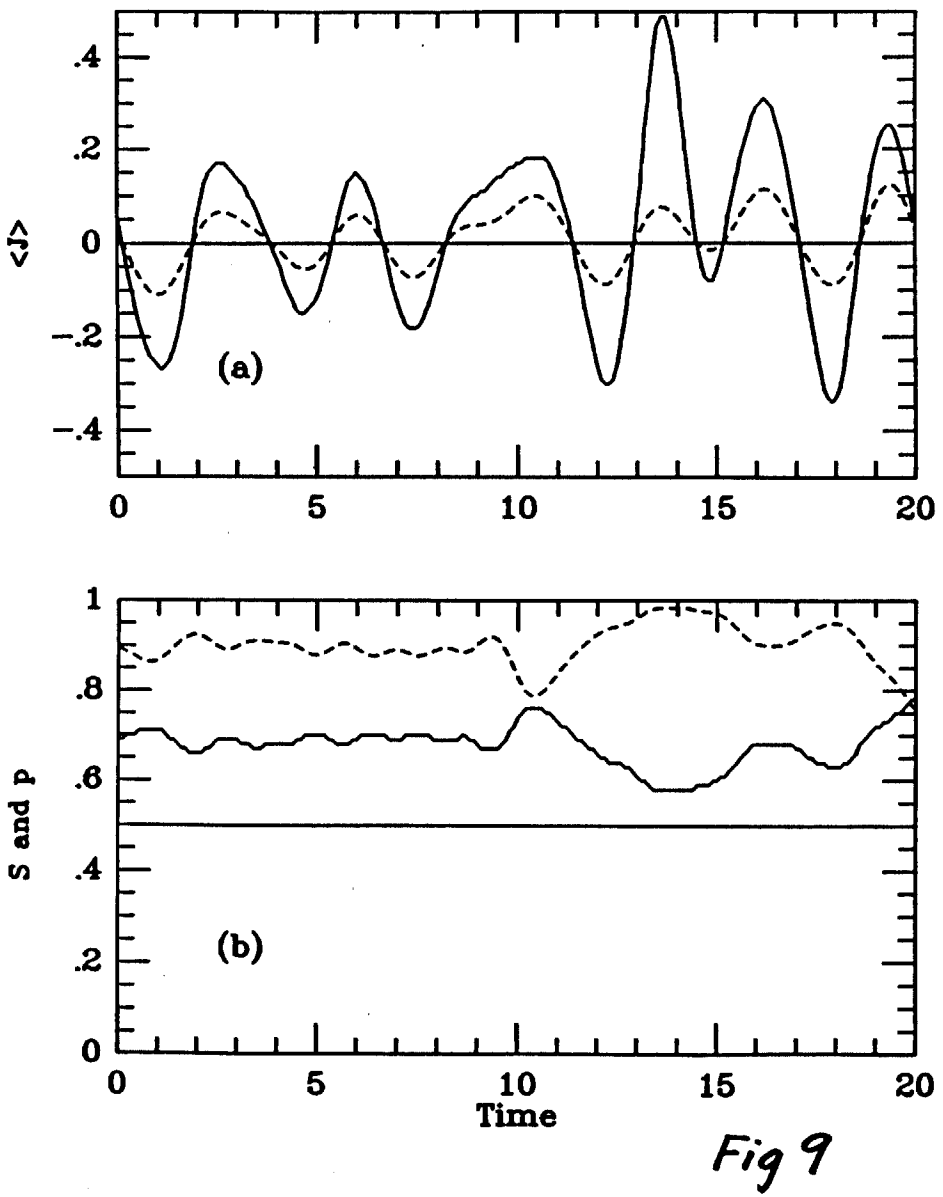
<J>
.4
.2
0
-.2
-.4
(a)
0
5
10
15
20
S and p
1
.8
.6
.4
.2
0
(b)
Time

Fig 9

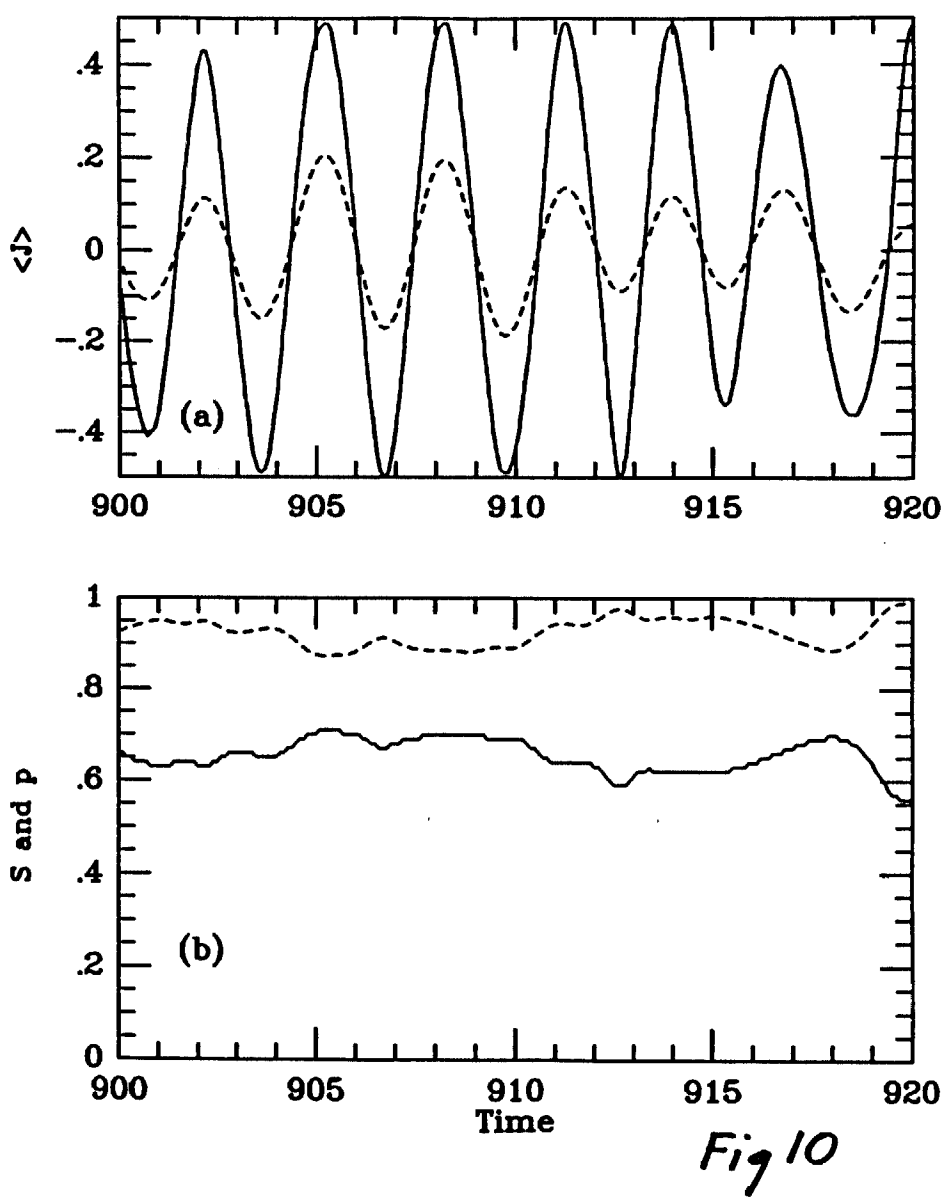
<J>
.4
.2
0
-.2
-.4
(a)
900
905
910
915
920
S and p
1
.8
.6
.4
.2
0
(b)
Time

Fig 10

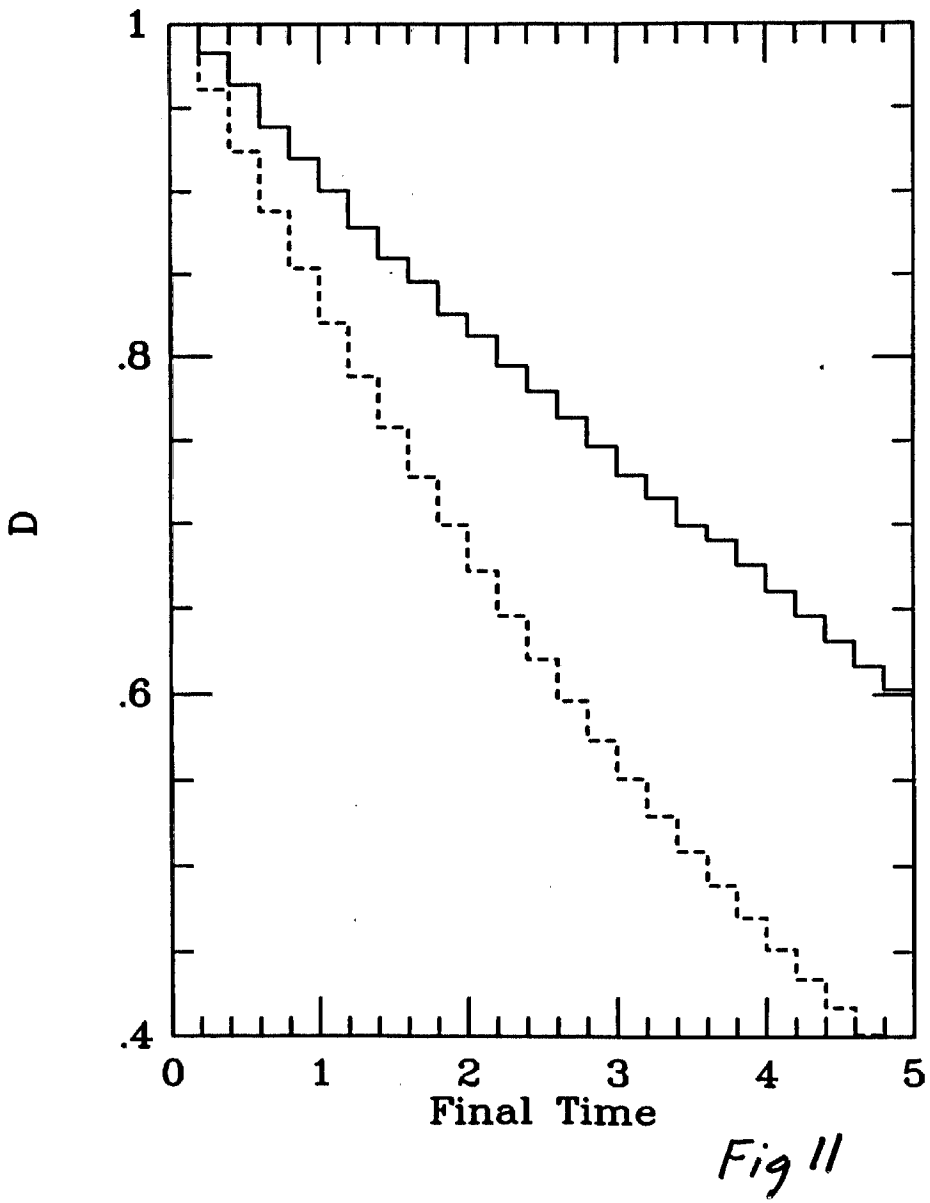

Fig 11

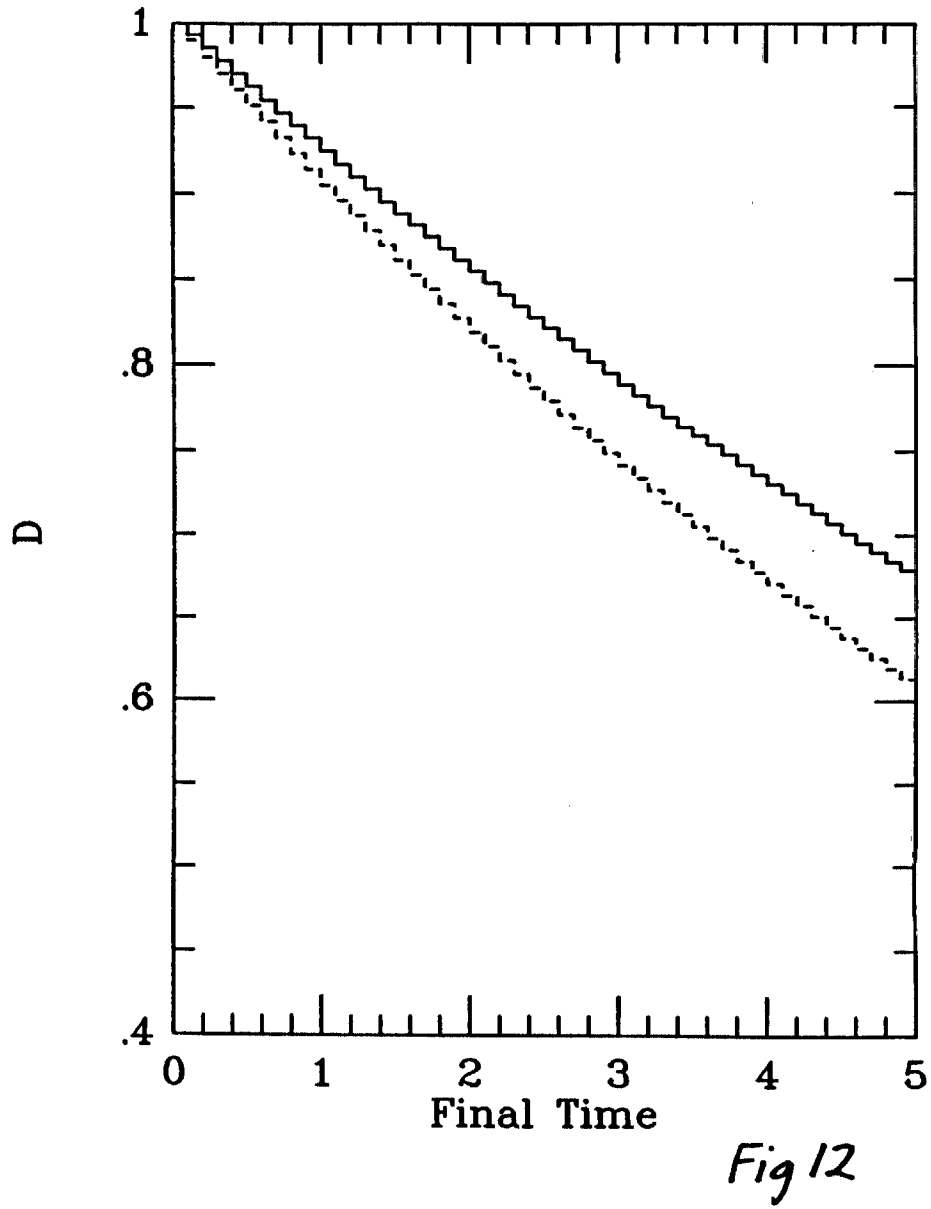

Fig 12

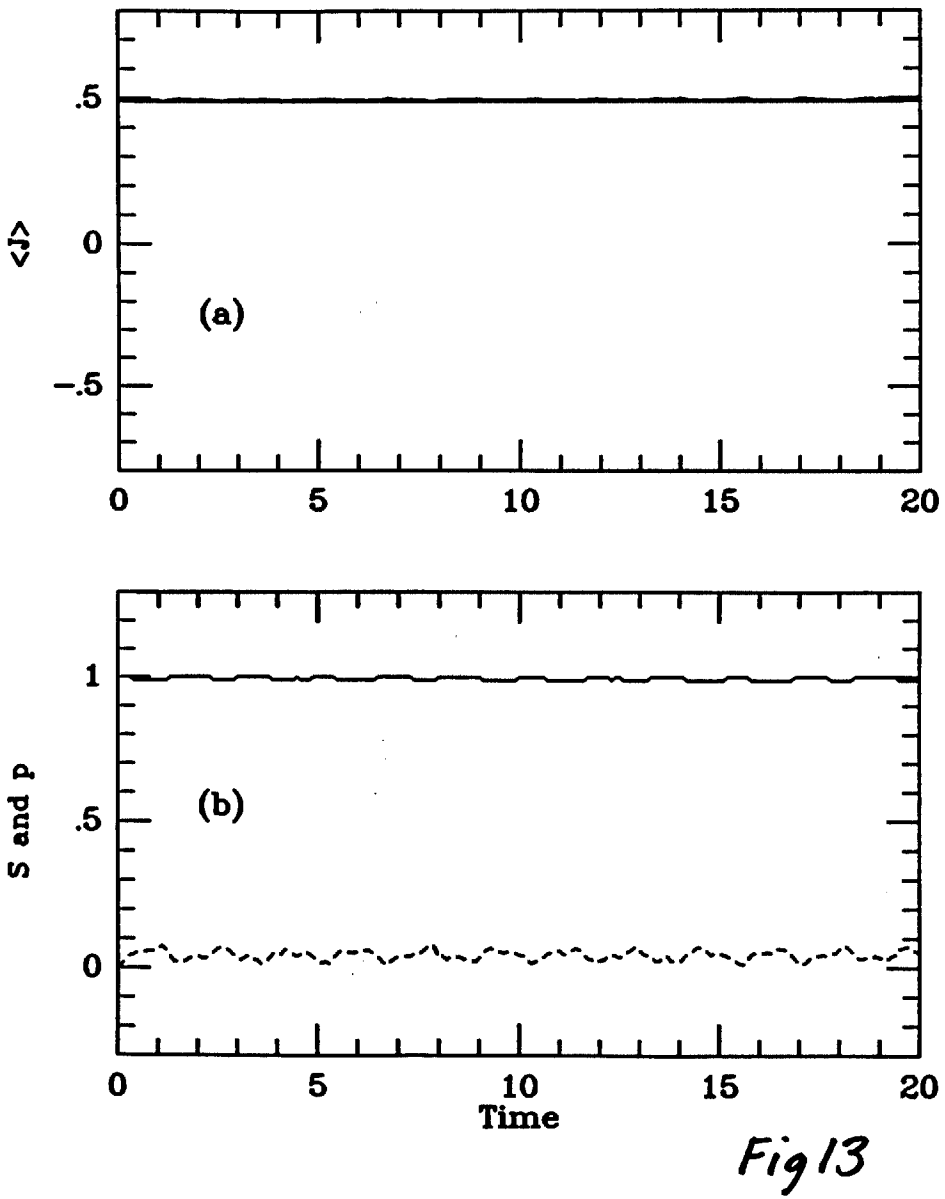
.5
0
-.5
<J>
(a)
0
5
10
15
20
1
.5
0
S and p
(b)
0
5
10
15
20
Time

Fig 13

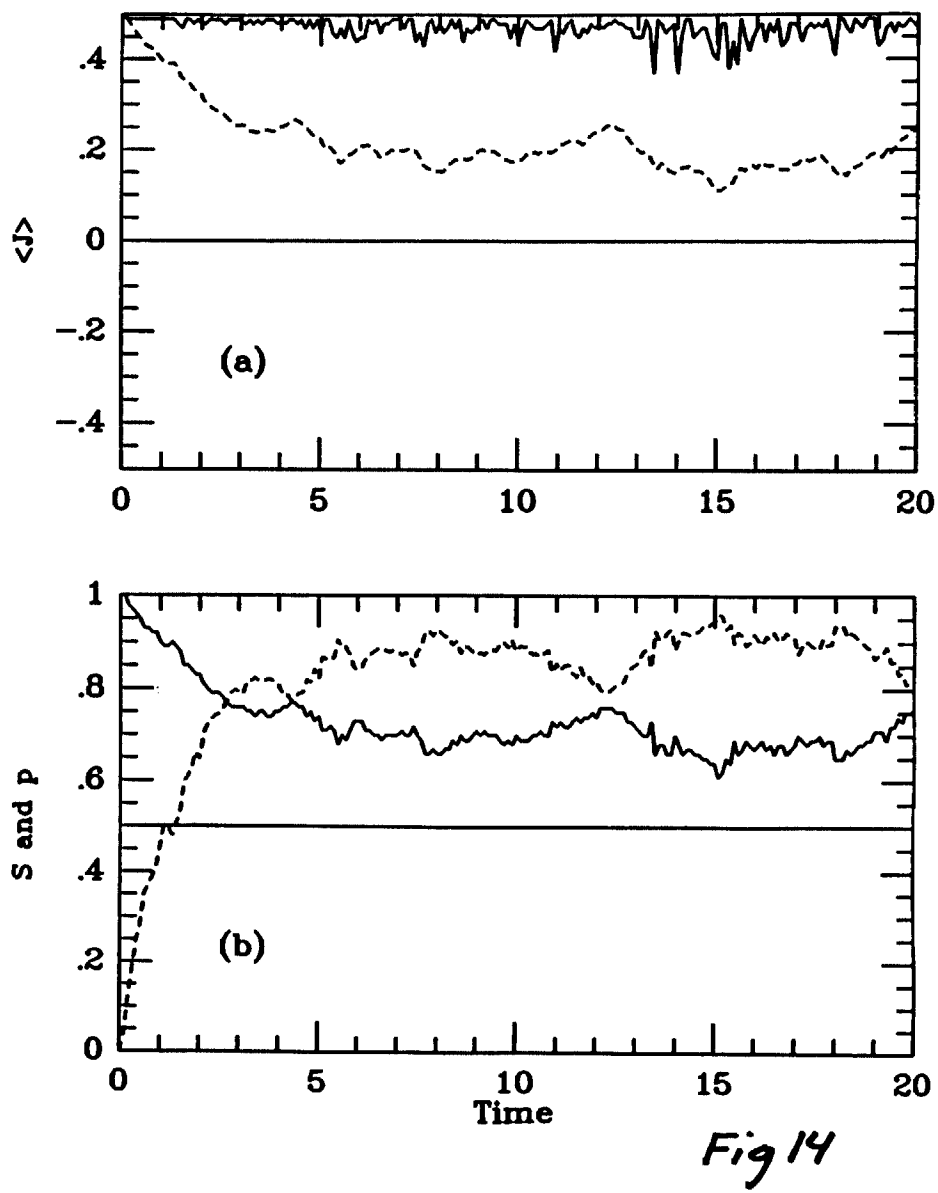
.4
.2
0
-.2
-.4
<J>
(a)
0
5
10
15
20
1
.8
.6
.4
.2
0
S and p
(b)
0
5
10
15
20
Time

Fig 14

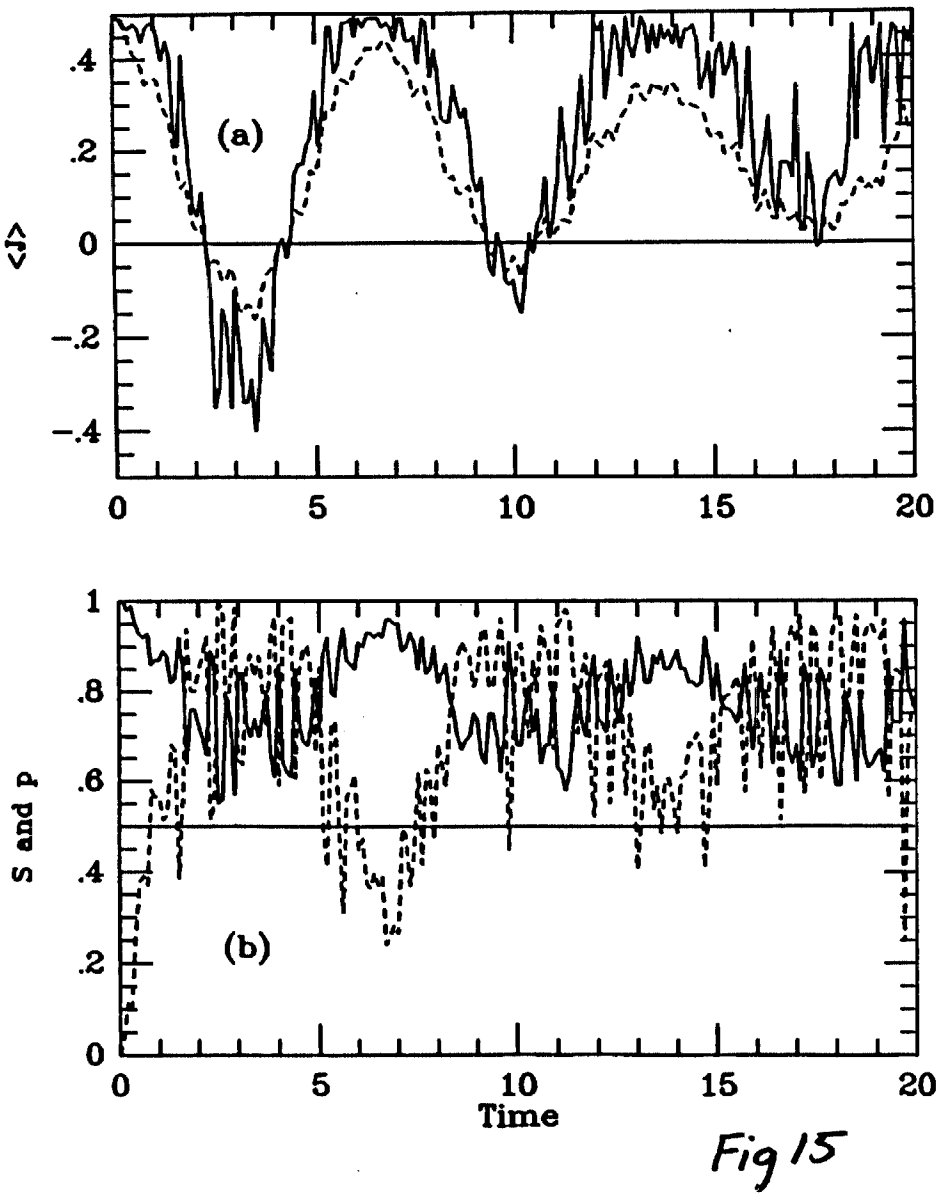
(a)
<J>
.4
.2
0
-.2
-.4
0
5
10
15
20
(b)
S and p
1
.8
.6
.4
.2
0
Time

Fig 15

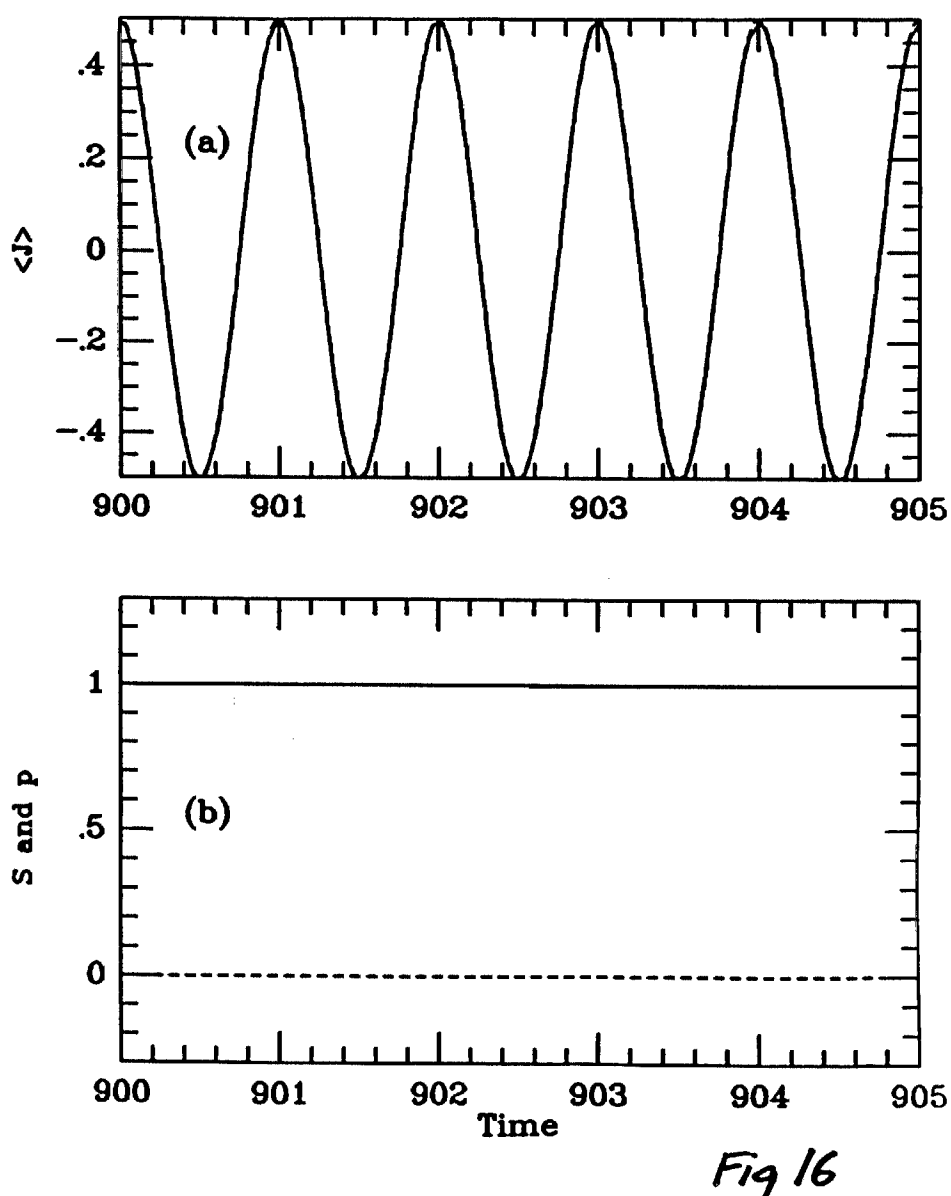
(a)
<J>
.4
.2
0
-.2
-.4
900
901
902
903
904
905
(b)
S and p
1
.5
0
Time

Fig 16